12-2023

The Discovery of Diverse Picophytoplankton Populations in the Columbia and Willamette Rivers Using Flow Cytometry

Kylee M. Lamberson
Portland State University, kbrevick@pdx.edu

The discovery of diverse picophytoplankton populations in the Columbia and Willamette Rivers using flow cytometry

by
Kylee Lamberson

An undergraduate honors thesis
submitted in partial fulfillment of the
requirements for the degree of

Bachelor of Science
in
Chemistry: Biochemistry

Thesis Advisor
Anne W. Thompson, Ph.D.

Portland State University
2023

Abstract

As important primary producers, picophytoplankton determine the flow of carbon and energy in aquatic ecosystems. Picocyanobacteria are one picophytoplankton group known to be dominant in oceans and lakes, but they are still poorly understood in river systems. This project examined picophytoplankton communities in two distinct river systems: the Columbia and Willamette Rivers in Portland, Oregon. I aimed to characterize and quantify the picophytoplankton populations in the context of the environmental conditions of the two rivers. I used flow cytometry to detect cells based on their relative size and pigment fluorescence. I sampled nearly weekly for ten months to capture population dynamics over seasonal changes and short-duration disturbances. And finally, I discovered seven distinct picophytoplankton populations present in both rivers at varying abundances over time. My findings highlight the physiological and genetic diversity that underlie these persistent and biogeochemically important primary producers in freshwater ecosystems.

Dedication

This thesis honors my grandmother, Connie Ferraer, who endured orphanhood with perseverance. The comprehensive viewpoint of this project mirrors her resilience and benevolence.

Acknowledgments

I am sincerely grateful to Dr. Anne Thompson for her guidance, mentorship, and substantial input in shaping this project. I am also thankful to Dr. Dirk Iwata-Reuyl for serving as a committee member. My appreciation extends to my lab mates and colleagues for their invaluable feedback throughout the research journey, particularly Dr. Yangdong Pan for his insights on environmental conditions. I am grateful to the BUILD EXITO Program staff for their unwavering support. A special acknowledgment goes to Dr. Eric Sheagley and Dr. Dean Atkinson for their belief in me since the beginning of my undergraduate research journey. Lastly, I want to convey my gratitude to the PSU Chemistry, Biology, and Environmental Science Departments for providing the resources necessary for me to pursue my academic interests and craft an Honors undergraduate thesis.

Funding was provided by the National Institutes of Health Common Fund and Office of Scientific Workforce Diversity under three awards, UL1GM118964, RL5GM118963, and TL4GM118965, for the BUILD EXITO Biomedical Research Training Program at Portland State University, administered by the National Institute of General Medical Sciences to KB. The work is solely the responsibility of the authors and does not necessarily represent the official view of the National Institutes of Health. Funding for laboratory supplies and instrumentation was provided by the NSF-OCE 1830002 and Simons Foundation LS-ECIAMEE-00001481 awards to Anne W. Thompson.

Table of Contents

List of tables

List of figures

Chapter 1

Introduction

Global energy and nutrient cycles are governed by microorganisms. The picophytoplankton are one microbial function group that contributes heavily to the carbon cycle via photosynthesis, a process by which sunlight energy is used to atmospheric carbon into aquatic ecosystems. The picocyanobacteria are one major subgroup of picophytoplankton. While picocyanobacteria have been well studied in oceans and large lakes (Stockner & Antia, 1986; Stockner, 1988), these tiny, carbon-fixing cells have yet to be studied carefully in river systems. River systems are important to microbial ecology because they connect the ecosystems that contain well-known picocyanobacteria populations. The goal of my thesis was to identify coexisting populations of picophytoplankton, such as picocyanobacteria, in major rivers. The populations were distinguished based on their unique pigment properties determined with flow cytometric measurements of relative forward light scatter and pigment fluorescence using different excitation lasers. I focused on two major rivers of the Portland Metropolitan region: the Columbia and Willamette. These rivers are distinct in several ways, making them an excellent natural laboratory for addressing questions of picophytoplankton ecology and biology. Ultimately, this has been the first study to investigate the picophytoplankton community structures that play a role in shaping each respective river system.

Biogeochemistry is driven by microorganisms

The flow of energy and nutrients on Earth is sustained via biogeochemical cycles. These components of biogeochemistry are released and stored through redox processes heavily influenced by microorganisms. The metabolisms of different microbial functional groups carry

out most of these redox reactions, thereby driving biogeochemical transformations on a global scale. Specifically, the evolution of highly conserved multimeric protein complexes in microorganisms provides a means for driving the biogeochemical cycling of hydrogen, carbon, nitrogen, oxygen, and sulfur (Falkowski et al., 2008, Kluyver & Donker, 1926; Williams, 1997).

A very important component of biogeochemistry is the carbon cycle. One major step in the carbon cycle is photosynthesis, which is the only known process of energy transduction that is not directly dependent on chemical bond energy (Falkowski & Godfrey, 2008). Instead, photosynthetic organisms use the energy from the sun to reduce carbon dioxide and oxidize water, producing organic carbon (biomass) and oxygen gas that is key for all life on Earth (Nelson et al., 2021). This makes photosynthetic organisms considered primary producers since they make carbon and energy available to other non-phototrophic species. The contribution of phytoplankton to aquatic ecosystems is also evident in the marine forms contributing roughly an equal amount of primary production per year as all land plants combined (Falkowski & Raven, 2000; Field et al., 1998).

Phytoplankton: picocyanobacteria

A significant component of phytoplankton communities are picophytoplankton, defined here as cells < 3 µm in diameter. Picophytoplankton include eukaryotic and prokaryotic microorganisms, like protists and picocyanobacteria, respectively. Picocyanobacteria are known primary producers in aquatic ecosystems around the globe, with identification and characterization done in marine, brackish, and freshwater lake systems (Callieri, 2010; Camacho et al., 2003; Ernst, 1991; Partensky et al., 1999a, 1999b; Pick, 1991; Stockner et al., 2000). The three most numerous types of aquatic primary producers are all picocyanobacteria, which

include *Prochlorococcus spp.*, *Synechococcus spp.*, and *Cyanobium spp.* (Partensky et al., 1999a, 1999b; Zwirglmaier et al., 2008), the latter two of which fall under the Synechococcales order. *Prochlorococcus* is only present in marine ecosystems while Synechococcales are found in marine, brackish, and freshwater ecosystems (Biller et al., 2015; Zwirglmaier et al., 2008). The ubiquitous abundance of these cells emphasizes their potential use as climate prediction tools. Future climate models show that shifts in biogeochemistry and food chain fluxes will be noticeable before phytoplankton populations go extinct (Dutkiewicz et al., 2021). For *Synechococcus spp.* in particular, a different niche model predicted these cells to increase in abundance by 14% with climate change (Flombaum et al., 2013). Thus, it is important to characterize these cells, to illuminate their ecological role in present and future scenarios.

One way to characterize picophytoplankton populations is by their size ranges. Cell size can determine the growth rate, nutrient affinity, and sinking habits of phytoplankton (Buitenhuis et al., 2008). Cell size is often viewed as a 'master trait' in ocean systems since it can dictate growth, sinking, and grazing pressure dynamics of phytoplankton communities, with some cell volumes recorded over nine orders of magnitude (Litchman et al., 2015; Ward et al., 2012). While some cells are larger than other cells, Synechococcales strains also may form microcolonies (Callieri et al., 2012; Jezberová & Komárková, 2007), thus becoming larger. New studies suggest that these microcolony formations can act as a defense mechanism against nanoflagellate predators (Callieri et al., 2016; Christoffersen, 1994; Jezberová & Komárková, 2007; Sanders et al., 2000; Stockner & Antia, 1986). Microcolony formations combined with adaptability to high and low temperature and sunlight levels results in Synechococcales' extreme plasticity in relieving environmental stressors (Callieri, 2017).

Another component of picophytoplankton communities, besides picocyanobacteria, are pigmented picoeukaryotes (Worden et al., 2004). Niche partitioning occurs between picocyanobacteria and pigmented picoeukaryotes in freshwater ecosystems (Cabello-Yeves et al., 2022; Callieri, 2017; Gale et al., 2023; Grébert et al., 2018; Haverkamp et al., 2009; Palenik, 2001; Six et al., 2007; Stomp et al., 2004; Winder, 2009). Thus, considering the entire picophytoplankton community, and identifying the contributions of these two phytoplankton groups, is important in aquatic microbial ecology. Since global air temperatures are projected to increase by 1.5-5 °C within the century (IPCC, 2001), this will lead to either the stabilization or inhibition of eukaryotic phytoplankton (diatoms, dinoflagellates, algae, etc.) while cyanobacteria abundances are predicted to increase (Paerl & Huisman, 2009). So, determining which populations are present and thrive under which environmental conditions is important for understanding the effects of climate change on aquatic ecosystems.

Flow Cytometry

Flow cytometry is an excellent technique for quantifying, characterizing, and sorting small, pigmented cells (Engh & Stokdijk, 1989; Moreria-Turcq et al., 1993; Olson et al., 1983, 1988; Stomp et al., 2004; Thompson & Engh, 2016; Wood et al., 1985). The hydrodynamic focusing of particles in aqueous samples ensures that one individual particle is analyzed at a time. Analysis involves the use of different lasers exciting each cell followed by the detection of forward light scatter and fluorescence. This flow cytometry method allows high throughput and precise analysis of individual cells as well as whole samples. From there, cells can be sorted for downstream genetic analysis purposes, with flow cytometry having been coined a “fingerprinting” technique for aquatic microbial samples (Koch et al., 2013).

The use of different excitation lasers is helpful when distinguishing between different fluorescence properties of cells. The most useful excitation wavelengths for distinguishing phytoplankton are 488 (blue) and 561 nm (green) lasers determined via multidimensional analysis of relative fluorescence action spectra using five different lasers, which corresponded to 18S rRNA phylogenetic analysis (Thompson & Engh, 2016). All photosynthetic microorganisms contain the green pigment, chlorophyll, while only some have an accessory pigment called phycoerythrin. These different pigment properties determine the different wavelengths of light that the microorganisms can harvest, with phycoerythrin-containing-cells likely being of Synechococcales descent (Olson et al., 1988; Thompson & Engh, 2016). Chlorophyll and phycoerythrin fluorescence wavelengths can be detected via flow cytometry at 642 ± 20 nm and 572 ± 13 nm, respectively (Thompson & Engh, 2016).

In flow cytometry, photosynthetic cells are typically distinguished from other particles and background noise by their chlorophyll fluorescence. Then, chlorophyll containing cells can be further distinguished from each other by looking at the chlorophyll detection via different excitation lasers. Phenotypic populations of cells plotted on bivariate plots of pigment fluorescence excited by different excitation lasers appear like elongated lines, which have been called “needles” (Thomspon & Engh, 2016). These needles are cells with the same pigment fluorescence ratios at different intensities, making the population distributions on bivariate plots an elongated, or needle-like, shape. By coupling cell sorting to sequencing, past work has determined that needles include cells with the same pigment properties, but different genotypes (Gale et al., 2023).

Flow cytometry is also effective at determining cell size. To determine the size of particles within a sample, forward light scatter detection can be used as a proxy for relative size with the aid of an internal polystyrene microsphere (bead) standard of known size. Mie theory has shown that the relationship between forward light scatter and size using flow cytometry is complicated and non-linear (Ribalet et al., 2019) and thus requires precise calibration. Despite the non-linear relationship, the forward light scatter detection can still be used to estimate the size range of picophytoplankton populations in reference to beads.

Phenotypic niche partitioning

The variation in eco-physiological traits among picocyanobacteria lineages is primarily associated with their pigment types (Callieri, 2010). Pigment composition can be used to characterize distinct strains of picophytoplankton based on the spectral niche that they fill (Grébert et al., 2018, 2022; Gale et al., 2023; Stomp et al., 2004), and even genetically related strains can have vastly different pigment compositions (Cabello-Yeves et al., 2022; Everroad & Wood, 2006; Gale et al., 2023; Scanlan & West, 2002). This variety in pigment types is thought to be due to horizontal gene transfer of pigment composition genes (Grébert et al., 2018, 2022). The main pigment types of *Synechococcus* spp. are referred to as Type 1, Type 2, and Type 3. Differences in phycobilisome composition among these pigment types are seen in the rods of light harvesting complexes consisting of one type of phycocyanin and/or two types of phycoerythrin (I and II). Type 1 *Synechococcus* have no phycoerythrin but do contain phycocyanin. Type 2 *Synechococcus* have phycoerythrin I and phycocyanin. And Type 3 *Synechococcus* have phycoerythrin I and II, and phycocyanin. The relative absorbance of these pigment types differs across the visible light spectrum with phycoerythrin I and II having slightly

different absorption spectra (Six et al., 2005, 2007). Thus, specific freshwater strains flourish by aligning their phycobiliprotein adsorption spectra with the prevailing light wavelengths (Callieri et al., 1996) in a process called photoacclimation. Therefore, it is crucial to classify these cells according to the ecological roles they play in capturing sunlight at various wavelengths.

While marine picophytoplankton communities are mostly represented by *Prochlorococcus* and *Synechococcus* genera, freshwater ecosystems contain far more diversity of picocyanobacteria, including *Synechococcus*, *Cyanobium*, *Synechocystis*, and *Cyanothece* genera (Cabello-Yeves et al., 2022; Crosbie et al., 2003; Sánchez-Baracaldo et al., 2008). The greater diversity of picocyanobacteria in freshwater environments ties into their genetic makeup as well. In comparison to marine strains, freshwater picocyanobacteria strains have larger genomes (2.9 Mb +/- 0.41 Mb) and %GC content (64% on average) (Cabello-Yeves et al., 2022). This greater genetic and phenotypic diversity alludes to a greater environmental adaptability. Therefore, connecting this vastly greater freshwater genome to the adaptability of picocyanobacteria populations is another area of importance that this thesis addresses.

Ecosystem dynamics

Concerning climate change, ecosystem models predict that changed environments will lead to changes in phytoplankton community structure (Dutkiewicz et al., 2015). While *Prochlorococcus* are the most abundant cells in our oceans, *Synechococcus* is the second most abundant in marine systems and the first most abundant, followed by *Cyanobium*, in freshwater systems (Sanchez-Baracaldo et al., 2005). Freshwater picophytoplankton communities (i.e., picocyanobacteria and pigmented picoeukaryotes) have been sufficiently studied in lakes (Cabello-Yves et al., 2022; Callieri, 2008; Ernst, 1991; Gale et al., 2023; Pick, 1991; Stockner et al.,

2000; Stomp et al., 2007) and estuary systems (Cabello-Yves et al., 2022; Callieri et al., 2012; Scanlan, 2012; Stomp et al., 2007; Wawrik & Paul, 2004), and until now, river systems. Specifically, while there is a known abundance of larger scale planktonic cells (e.g., diatoms) within the Columbia and Willamette Rivers (Prahl et al., 1997; Small & Morgan, 1994; Sullivan, 1997; Sullivan et al., 2001), as well as picocyanobacteria cells documented within the Columbia Estuary (Frame & Lessard, 2009; Haertel et al., 1969; Jones et al., 1990), this will be the first study to phenotypically distinguish between these cells within the flowing freshwater ecosystems of Portland, OR.

The confluence of the Columbia and Willamette Rivers is located at the northern/northwestern tip of Portland, Oregon. At this convergence, the Willamette River flows into the Columbia River, which is the largest river in the Pacific Northwest region of North America (USGS, 1990). Understanding how the phytoplankton in these rivers contribute to the marine ecosystem is important in connecting the freshwater realm to the saltwater realm of the photosynthetic microbiome. This ecological relationship is dynamic with high gradients of environmental parameters such as temperature, light, and nutrient availability affecting phytoplankton growth and primary productivity across marine (Chisholm, 1992) and freshwater ecosystems (Vörös et al., 1998).

Phytoplankton growth depends on the balance between temperature, nutrients, and light. Temperature increases are known to contribute to phytoplankton growth (Lewandowska et al., 2012; Rose & Caron, 2007). Yet, when surface ocean water temperatures reach above 14 °C, nitrate concentrations are low and become a limiting factor (Li, W. K. W., 1998). However, nutrient limitations on phytoplankton growth have been reopened for debate, since it remains

unclear whether nitrogen or phosphorus are the limiting factor in marine and freshwaters systems (Callieri, 2010). Despite this debate, phytoplankton growth can be attributed to either temperature, light, or nutrients depending on the time of year and the ecosystem conditions.

Turbidity is another parameter in rivers that could influence phytoplankton growth. While the measurement of turbidity accounts for all particles scattering light (Swanson & Baldwin, 1965), this measurement has been shown to consist primarily of suspended detrital minerals (i.e., sediment) in the Columbia River (Sullivan et al., 2001). Additionally, the waters of the Columbia River may be less turbid than the Willamette River, due to the dams slowing the flow of the river, thus causing less upwelling of sediment (Sullivan et al., 2001). Essentially, less turbid waters allow for more sunlight to reach phytoplankton, leading to more growth (Nolan, 2018; Sullivan et al., 2001).

The discharge of a river, measured as the flow rate over time (Bongard, 2018), is another parameter that can be used to gauge how well the two ecosystems support phytoplankton growth. Dramatic fluctuations in discharge in river systems, likely due to dam operations or heavy rainfall, can cause the upwelling sediment leading to increased turbidity. Therefore, discharge can also affect phytoplankton growth regarding sunlight availability as discussed previously. With that, primary production can be limited by water retention time and light availability due to vertical mixing (inferred from relative changes in discharge) and turbidity dynamics of river ecosystems (Sullivan et al., 2001).

Summary

This study is the first to examine the community structure of picophytoplankton within the Columbia and Willamette Rivers just before the confluence. I used a high-resolution sampling

method corresponding to continuously measured hydrological data provided by USGS. This project aims to answer the following questions regarding picophytoplankton communities within the flowing freshwater ecosystems of Portland, Oregon: (1) How many different phenotypic populations are present in each river? (2) Do these populations abundances shift over time, and if so, how might they differ between the two rivers? (3) Are these two rivers different in terms of supporting different picophytoplankton communities?

To address these questions, I designed and executed a 10-month long surface water sampling regime in Portland's rivers to identify picophytoplankton populations. I used flow cytometry to analyze samples taken from the Columbia and Willamette Rivers about every week from September 2022 to July 2023. Different populations of picophytoplankton cells were characterized via relative pigment fluorescence. Then, the concentration (cells per mL) of each population in every sample was assessed over the period. The environmental conditions of each river were also compared to make sense of picophytoplankton abundance patterns. Future work will statistically quantify the ecological relationship by determining how strongly changes in different picophytoplankton population abundances correlate with changes in environmental factors.

Chapter 2

Materials and methods

Research approach overview

A summary of the research approach for this study is shown in Figure 1. Surface water samples were taken roughly every week from separate locations along the Columbia and Willamette Rivers in Portland, Oregon. These samples were fixed, flash frozen, and stored for later analysis. Flow cytometry was used to analyze cells within every sample based on relative size and pigment fluorescence. Population data was distinguished using the software *FlowJo*. Retrieval of USGS station hydrological data was visually assessed in comparison to population abundances over time.

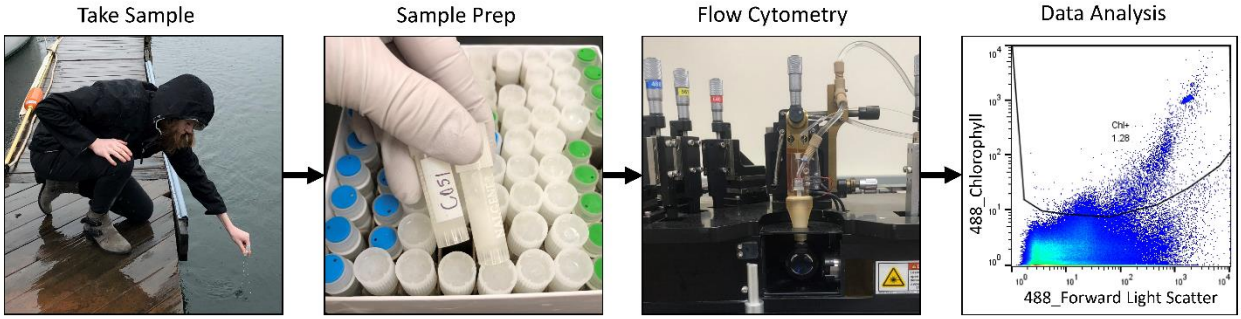

Figure 1. Methodology flow chart. From left to right, the images are as follows: grab sampling, the frozen samples stored in cryotubes, the flow cytometry interrogation chamber, and an example plot of the gating process. The right-most image consists of a colored density dot plot, with high numbers of overlapping cells (i.e., dots) in bright blue, corresponding to the relative forward light scatter and chlorophyll fluorescence of each cell excited by blue light (488_Chlorophyll vs. 488_Forward Light Scatter). The gate drawn (black line) encompasses chlorophyll-containing cells (CHL+).

Sample collection

Surface water samples were collected at two locations in the river systems of the Portland Metropolitan Region, approximately weekly from September 2022 until July 2023 (Figure 2). The sampling site in the Columbia River was located at the Bridgeton Moorage private dock

(45.60237, -122.66056) roughly 10 km upriver of the Columbia and Willamette confluence (45.65716, -122.76369) that is around 150 km upriver of the Columbia River Estuary. The sampling site in the Willamette River was located at the Riverplace Marina public dock (45.51045, -122.67183) roughly 20 km upriver of the Columbia and Willamette confluence. These two locations were ideal for grab sampling the surface water off each dock by hand. Collection water was obtained using 15 mL centrifuge tubes, which were rinsed with river water three times before keeping 15 mL. At one time point, multiple samples were taken along multiple locations of each dock to measure the variability in cell abundance based on sampling location.

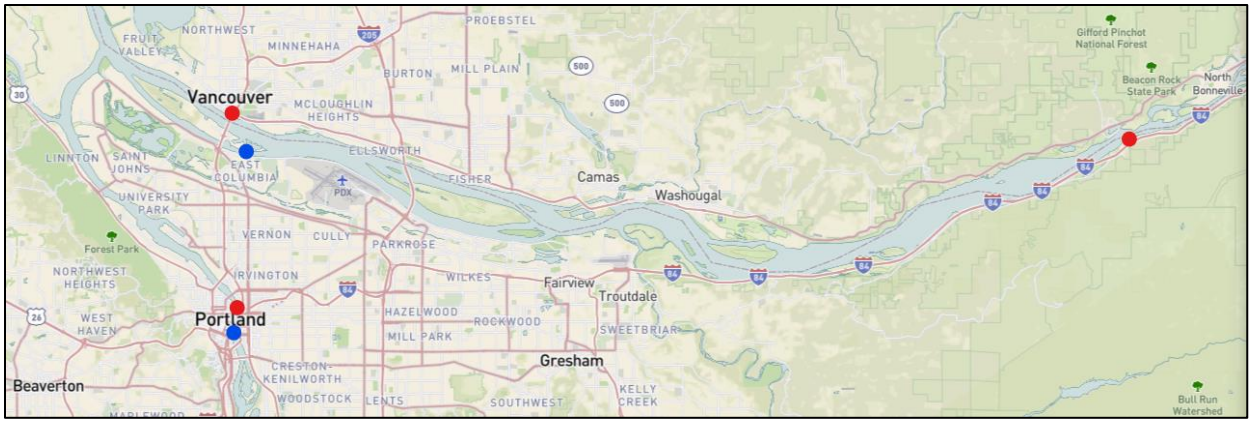

Figure 2. Sample sites (blue) in comparison to USGS data retrieval sites (red). The sampling site along the Columbia River was off a private dock along the inner channel of Hayden Island, with two USGS sites used for data retrieval: #14144700 off the shore of Vancouver, WA and #453630122021400 just west of Bonneville Dam. The sampling site along the Willamette River was off the Riverplace Marina public dock with the USGS site location #14211720 just downstream off the Morrison Bridge.

Sample storage and preparation

Three 1 mL replicates (one each for analysis, cell sorting, and as back-up) of each 15 mL river water sample were fixed using 10 µL electron microscopy grade glutaraldehyde (25% aqueous solution; Electron Microscopy Sciences, Hatfield, PA). Replicate samples were incubated in the dark for approximately 10 minutes and then flash frozen using liquid nitrogen. Samples were stored at -20 °C awaiting analysis.

To prepare frozen samples for flow cytometry, one replicate of each river sample was thawed. Thawed samples were prefiltered using 50 µm disposable filters (Partec North America, Swedesboro, NJ), to remove large particles. 5 µL of each internal standard (UltraRainbow 3.8 or 4.1 µm diameter, Catalog No. URFP-38-2, Spherotech, Lake Forest, IL; Yellow Green 1.00 µm diameter, Catalog No. 17154-10, Polysciences, Inc., Warrington, PA) were added to 900 µL of each filtered sample. Filtered samples containing beads were ready for flow cytometric analysis once vortexed to ensure homogeneity throughout.

Flow Cytometry Analysis

A BD Influx cell sorter (BD Biosciences, San Jose, CA) equipped with three lasers (488, 561, 692 nm), an 80 µm diameter nozzle, a small particle detector, and photomultiplier tubes (PMTs) was used for flow cytometric analysis. A block diagram schematic of the flow cytometer used is shown in Figure 3. Flow cytometry sheath solution (BioSure®, Grass Valley, CA) was used as the sheath fluid. The instrument flow rate was measured each day of analysis by weighing replicate blanks (DI water) before and after running them through the flow cytometer for at least 4 minutes. The flow rate (volume per time) was then calculated by taking the difference in water weight (1 g = 1 mL) divided by the time the sample was ran. Sample flow rates ranged from 0.314 to 1.41 µL per second. The analyzed volume of each sample was determined by tracking the time each sample was ran and applying the flow rate from their respective analysis days, resulting in a value of cells per volume of each sample.

Data collection was triggered on forward light scatter excited by the 488 nm laser using BD Sortware (BD Biosciences, San Jose, CA) for every event (i.e., particle or cell) in a sample. Chlorophyll *a* (CHL) fluorescence was detected using 692/40 nm bandpass filters for each PMT

corresponding to all three lasers. Phycoerythrin (PE) fluorescence was detected using 572/27 nm bandpass filters for each PMT corresponding to only the blue (488 nm) and yellow green (561 nm) lasers. Ultra Rainbow (UR; 3.8 or 4.1 µm diameter, Catalog No. URFP-38-2, Spherotech, Lake Forest, IL) and Yellow Green (YG; 1.00 µm diameter, Catalog No. 17154-10, Polysciences, Inc., Warrington, PA) beads were used for laser alignment as well as an internal reference for gating.

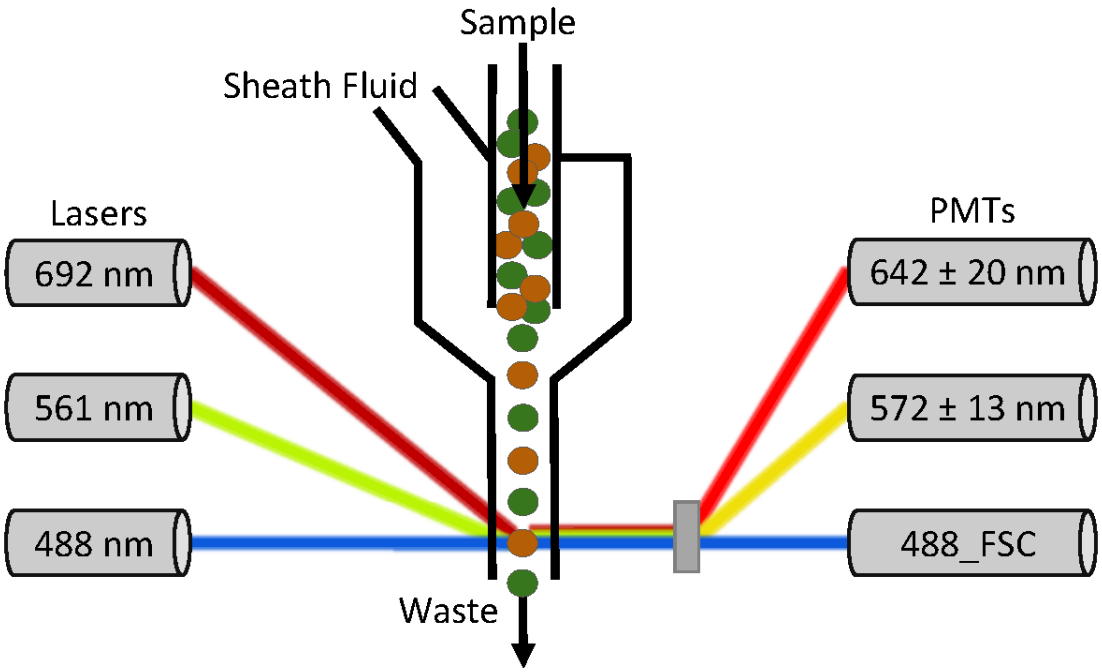

Figure 3. Block diagram schematic of the flow cytometer. Sample injection is surrounded by sheath fluid, and the cells are hydrodynamically focused by the nozzle shape to form a single line of cells passing the laser to facilitate single-cell analysis. Lasers of different wavelengths (488 nm, 561 nm, and 692 nm) excited the pigments of the cells. Forward light scatter excited by the 488 nm laser (488_FSC) was used as a proxy for size. Bandpass filters allowed the photomultiplier tubes to detect ranges of fluorescence wavelength, corresponding to chlorophyll fluorescence (642 ± 20 nm) and phycoerythrin fluorescence (572 ± 13 nm) excited by all three lasers.

Gating is the classic flow cytometric data analysis method to quantify and identify like cells that compose phenotypic populations. A hierarchical gating strategy (Figure 4A) was applied to every sample. Flow cytometric graphics (Figure 4B,C) were created using FlowJo (BD Biosciences, San Jose, CA). Figure 4A demonstrates the gates that were created and named as

follows. First, cells that contained CHL, coined “chlorophyll positive”, were determined via bivariate plots of forward light scatter and CHL fluorescence excited by the 488 nm laser (488_FSC vs. 488_CHL) to be events with 488_CHL greater than the background noise (Appendix A). Next, the internal bead standards were gated and removed from the CHL positive cell count via bivariate plots of PE fluorescence excited by 488 and 561 nm lasers (488_PE vs. 561_PE), since these parameters were able to capture both the UR and YG beads within one gate without including cells.

The CHL positive cells were first distinguished as containing medium to high or low levels using bivariate plots of CHL fluorescence excited by the 488 and 561 nm lasers (488_CHL vs. 561_CHL). The medium to high CHL cells were further gated into three subgroups using the same bivariate plots of 488_CHL vs. 561_CHL. Group 1, Group 2, and Group 3, and the low chlorophyll group each consisted of subpopulations that were further distinguished as distinct non-overlapping populations using bivariate plots of 488_PE vs. 561_PE. Populations that contained medium to high levels of CHL and/or PE were designated “C”, “P”, or “CP”. Naming of flow cytometry populations has been a challenging task in many marine systems (Thyssen et al., 2022), with a greater variety of cells identified in this freshwater system of the Columbia and Willamette Rivers. Thus, this simple naming scheme was inspired by Gale et al. (2023) that did not assume size or genetic makeup of the cells in each population.

Population gates were used to obtain a cell count for each population present in each sample. The concentration of CHL positive cells as well as each of the seven populations was calculated by dividing the number of cells by the sample volume analyzed. The abundance of CHL positive cells over time was plotted using the package ‘ggplot2’ (Wickham, 2016) in R (version

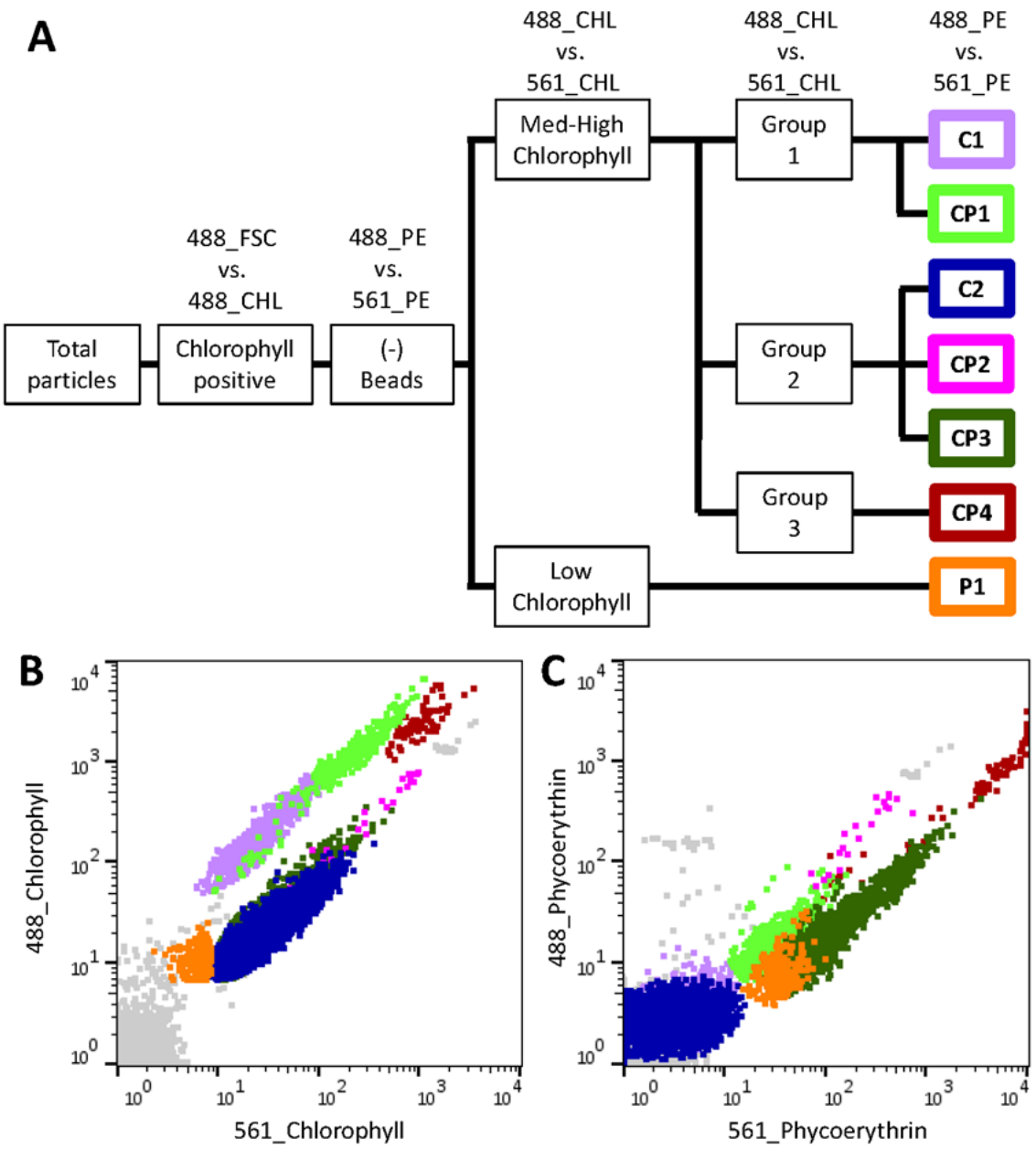

Figure 4. Gating scheme for differentiating coexisting populations of picophytoplankton based on pigment fluorescences analyzed via flow cytometry. A) Starting with total particles, the forward light scatter and chlorophyll detection via the 488 nm laser (488_FSC vs. 488_CHL) were used to determine chlorophyll-containing cells (chlorophyll positive). The interna standards (beads) were best identified using phycoerythrin detection via the 488 and 561 nm lasers (488_PE vs. 561_PE). Cell populations were first grouped as low or med-high chlorophyll fluorescence using chlorophyll detection via the 488 and 561 nm lasers (488_CHL vs. 561_CHL, plot B). The med-high chlorophyll populations were further divided into three groups also based on the 488_CHL vs. 561_CHL parameters (plot B). Each of the three med-high chlorophyll groups plus the low chlorophyll group were further distinguished using phycoerythrin detection via the 488_PE vs. 561_PE parameters (plot C). Cells are color-coded by their final population designation. Note that plots B and C represent the same sample taken from the Columbia River on July 18, 2023.

4.2.1, R Core Team, 2021) to assess the overall picophytoplankton communities in each river (see results Figure 5). Then, the abundance of each population was visualized using the R package 'pheatmap' (version 1.0.12; Kolde, 2019) to display the log scale of the concentration of cells corresponding to each phenotype shown in Figure 4 over the sampling period (see results Figure 7).

Environmental data retrieval

The U.S. Geological Survey (USGS) provides publicly available hydrological data at different points along the Columbia and Willamette Rivers, which was used for the environmental context of this study. Continuous and daily average readings were retrieved from USGS sites within the study region, and on the two rivers, using the R package 'dataRetrieval' (version 2.7.13; De Cicco et al., 2023). The three data parameters available in both rivers were discharge (cubic feet per second, cfs), temperature (°C), and turbidity (Nephelometric Turbidity Units, NTU). Nitrate data, measured as mg per L of nitrogen, was only available from the Willamette River. The closest USGS station to the Columbia sampling site was off the shore of Vancouver, WA (site #14144700) and provided discharge and turbidity data. The next-closest USGS station was located just after the Bonneville Dam (site #453630122021400) and provided temperature data. Since the latter site is located after the dam, it was determined to be the best available representation of what water temperatures may contribute to sampling downriver. The closest USGS station to the Willamette sampling site was just downriver off the Morrison Bridge (site #14211720) and provided all four data parameters mentioned previously.

Chapter 3

Results

Identification of picophytoplankton

To identify unique populations of the smallest photosynthetic cells, I applied hierarchical gating to the flow cytometry data. The first step of the hierarchical gating strategy defined chlorophyll-containing (CHL+) cells (relative red fluorescence > 10, Appendix B) that were roughly ≤ 4.0 µm (see size distribution of cells Figure 6). In this way, I identified these CHL+ cells as picophytoplankton.

To understand the temporal dynamics of the picophytoplankton communities in each river, I examined the concentration of CHL+ cells per mL over time between both sample sites (Figure 5). The picophytoplankton accounted for less than half of the total particles detected via forward light scatter in each sample (Appendices A & B). Both rivers showed a similar trend of decreasing and increasing picophytoplankton concentrations from September to January and from January to July, respectively. One major difference is that the Columbia River had a late September bloom, recorded on September 27, 2022, of about 17,000 cells per mL, which was not observed at the Willamette site. This peak dropped and decreased until December, with the lowest abundance of picophytoplankton recorded on November 10, 2022, in the Columbia River. Then, the picophytoplankton community increased in abundance again by the summer with another bloom recorded on June 15, 2023, of about 40,000 cells per mL.

The Willamette River had a similar trend to the Columbia River in its shifts of picophytoplankton concentration over the sampling timeframe. A bloom in the Willamette recorded on September 22, 2022, reached upwards of 25,000 cells per mL and was about half

the number of cells in the Columbia at this time. This picophytoplankton community dropped and peaked throughout the winter months in the Willamette River, with another small bloom recorded on December 30, 2022, that was a little less than 25,000 cells per mL. From there the picophytoplankton community was less abundant in the Willamette River than in the Columbia River between January and May. And finally, a massive bloom appeared in the Willamette in July, surpassing both blooms seen in the Columbia recorded over 60,000 cells per mL on July 18, 2023.

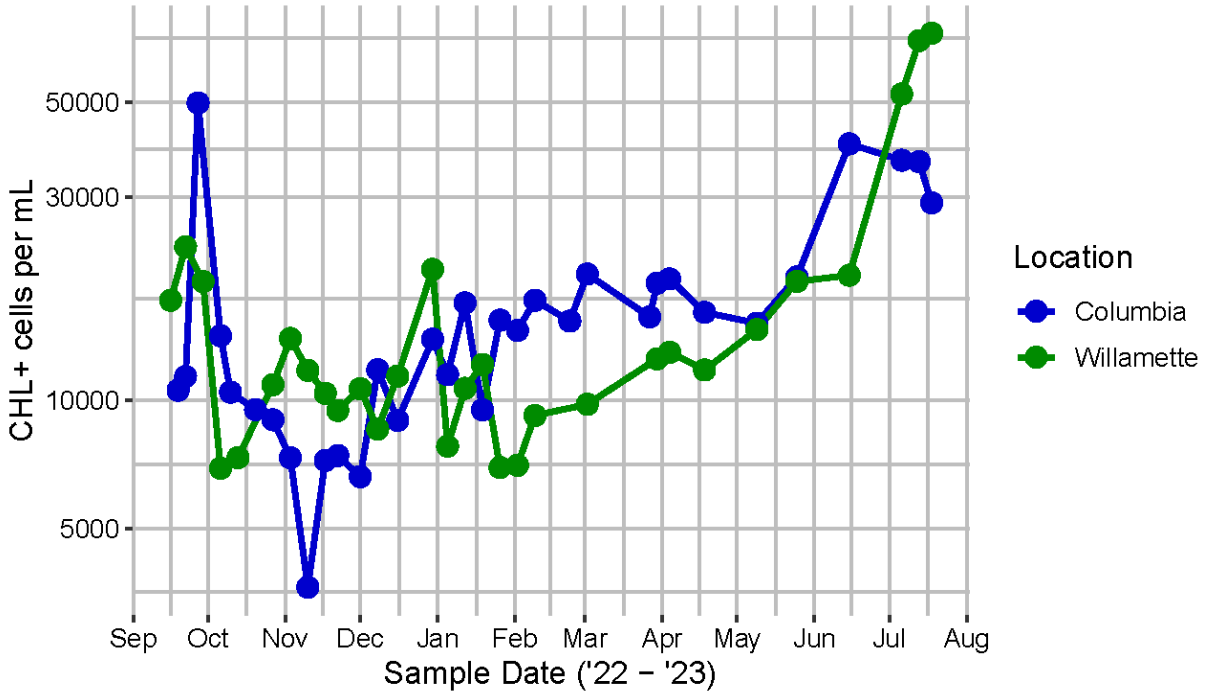

Figure 5. The concentration in cells per mL of chlorophyll-containing cells (CHL+) over the sampling timeframe for both rivers. Note the y-axis is a logarithmic scale.

Phenotypic diversity within the picophytoplankton

To see if there were coexisting subpopulations among the picophytoplankton, I further separated the chlorophyll positive cells based on their chlorophyll and phycoerythrin fluorescence under different laser excitations. Ultimately, I identified 7 populations of picophytoplankton.

The unique fluorescence intensities of these populations (Figure 4B,C) are similar to phenotypic needles that have been observed with Synechococcales and eukaryotic phytoplankton of different pigment types (Thompson & Engh, 2016). These populations, also termed “flow phenotypes”, contained cells with similar sizes and pigment fluorescence ratios (Gale et al., 2023). In most cases, there were subpopulations within the chlorophyll needles that were defined by assessing phycoerythrin fluorescence. In some instances, the populations could not be gated with confidence (i.e., overlapping or inconsistent distributions), so those cells were not part of any defined population. Specifically, the CP4 population contained subpopulations that were inconsistent in their fluorescence levels between samples, thus it was not gated further. A detailed description of each flow phenotype is as follows.

Two populations had relatively medium to high levels of chlorophyll fluorescence with little to no phycoerythrin fluorescence (designated “C” populations). These two populations, C1 and C2, exhibited parallel needles in the bivariate chlorophyll fluorescence plots (Figure 4B,C). C1 had higher levels of chlorophyll fluorescence excited by the 488 nm laser than C2. Viewing C1 and C2 on a bivariate phycoerythrin fluorescence plot did not result in needle formations and instead round-shaped distributions.

Four of the populations contained medium to high chlorophyll and phycoerythrin fluorescence (designated “CP” populations). CP1 was an elongated needle distribution in the bivariate chlorophyll fluorescence plots that shared a ratio with C1, but with greater chlorophyll fluorescence. Viewing CP1 on the bivariate phycoerythrin plots resulted in a slightly shorter and wider distribution that was somewhat parallel to CP3 (Figure 4B,C). CP2 had a smaller number of cells that spanned a shorter range of fluorescence, parallel to CP1 on the bivariate chlorophyll

fluorescence plots. CP2 had similar chlorophyll fluorescence ratios to C2 and CP3, but with higher fluorescence. Viewing CP2 on bivariate phycoerythrin fluorescence plots showed that this population had a similar phycoerythrin fluorescence ratio to CP1, but with higher fluorescence.

CP3 was an elongated distribution in both bivariate plots of chlorophyll and phycoerythrin fluorescence. CP3 shared a similar chlorophyll fluorescence ratio with C2, being parallel to C1 and CP1. In contrast, CP3's phycoerythrin fluorescence ratio was parallel to CP1 and similar to P1, but with greater phycoerythrin fluorescence. CP4 had a slightly rounder distribution in the bivariate chlorophyll fluorescence plots in comparison to the other needles but had the highest chlorophyll fluorescence overall. From there, CP4 contained inconsistent subpopulations that were revealed in the bivariate phycoerythrin plots; thus, these possible subpopulations were not gated. CP4 contained the highest phycoerythrin fluorescence as well.

Just one population had relatively very low levels of chlorophyll, yet detectable phycoerythrin fluorescence (designated "P"). While P1 chlorophyll fluorescence was low, these cells were still distinguishable from the background noise in most samples. However, in some samples P1 was indistinguishable from noise and thus not considered in the temporal abundance analysis (see temporal dynamics section, Figure 7). The samples that had distinguishable P1 populations were further discriminated from noise in the bivariate phycoerythrin plots, which showed P1 sharing a phycoerythrin fluorescence ratio with CP3, parallel to CP1. P1 was a round-shaped distribution in both bivariate pigment fluorescence plots.

Size distributions of cells

I used the forward light scatter, relative to the internal bead standards, to estimate each population's cell size range and average (Figure 6). C1, C2, CP1, CP2, and CP3 all had an additional bump on the right of their forward light scatter distributions, indicating a greater size range for these populations composed of larger cells or microcolonies. For instance, the mean of CP1 cells was smaller than the 4.1 µm beads, but some cells from the population were larger (i.e., a long-tailed distribution to the right). The C1 mean was smaller than CP1, with some of its larger cells overlapping with the smallest cells of CP1. CP3 cells were among the smallest of the populations, being slightly larger than the 1.0 µm beads. The CP3 distribution also had a tail to the right with a small peak of cells roughly the same size as the average C1 cells.

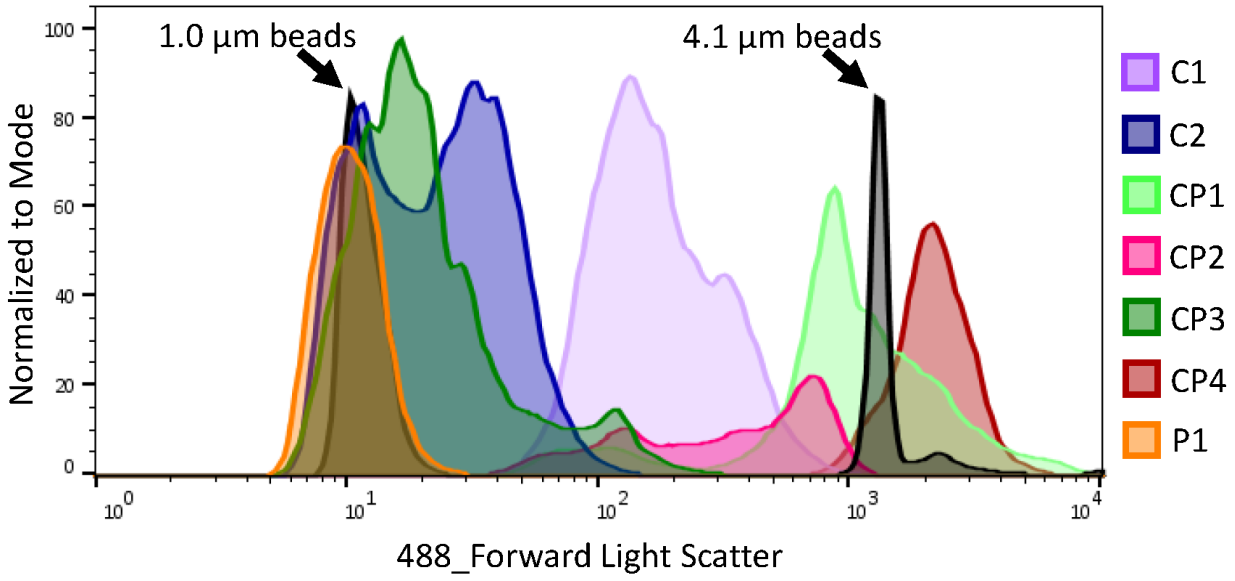

Figure 6. Histogram displaying the relative forward light scatter excited by the 488 nm laser of each population compared to the internal bead standards. The 1.0 um beads' peak is directly behind P1, averaging around a forward light scatter value of about 10. The 4.1 um beads' peak average is around 10^3. The seven populations are labeled on the right, colored as in Figure 3. The forward light scatter detection was used as a proxy for relative size ranges for each population. Note the x-axis is a log scale.

Populations C2 and CP2 were bimodal in their size distributions. C2 was composed of cells that were just slightly larger than the 1.0 µm beads plus cells that were larger than the average CP3 cell. In comparison, CP2 cells were mostly the same size as the average CP1 cell, but also had a significant number of cells that were the same relative size as the larger CP3 cells.

The mean cell size of each population was inferred from forward light scatter excited by the 488 nm laser relative to 1.0 µm and 4.1 µm internal bead standards (Figure 6). The 1.0 µm beads had a normal distribution averaging around a forward light scatter value of 10 and being directly behind population P1 on the plot. The 4.1 µm beads had a mostly normal distribution that had a short tail to the right, indicating the detection of beads that stuck together (a common phenomenon in flow cytometry), increasing their relative size. CP4 forward light scatter averaged higher than the 4.1 µm beads, indicating that they are slightly greater than or equal to 4.1 µm. CP1 forward light scatter peaked slightly lower than the beads but was skewed to the right as well, overall ranging from 10^2 to 10^4. C1 and CP2 forward light scatter covered a similar range from less than 10^2 up to 10^3, yet peaking around 10^2 and 10^3, respectively. C2 and CP3 forward light scatter covered similar ranges from about 10 to 10^2, with both being relatively smaller than the forward light scatter ranges of C1 and CP2. CP3 peaked around a forward light scatter value of 10, while C2 had two peaks at 10 and closer to 10^2. Lastly, P1 had the lowest levels of forward light scatter detection averaging a value of about 10.

Temporal dynamics

In order to see if these picophytoplankton subpopulations responded differently to environmental conditions, I compared their abundance over time in both rivers (Figure 7). First, I showed that the seven different populations were present in both the Columbia and Willamette Rivers. Second, while there were similar trends between populations of the two rivers, I showed that the temporal dynamics of each population was unique over space and time.

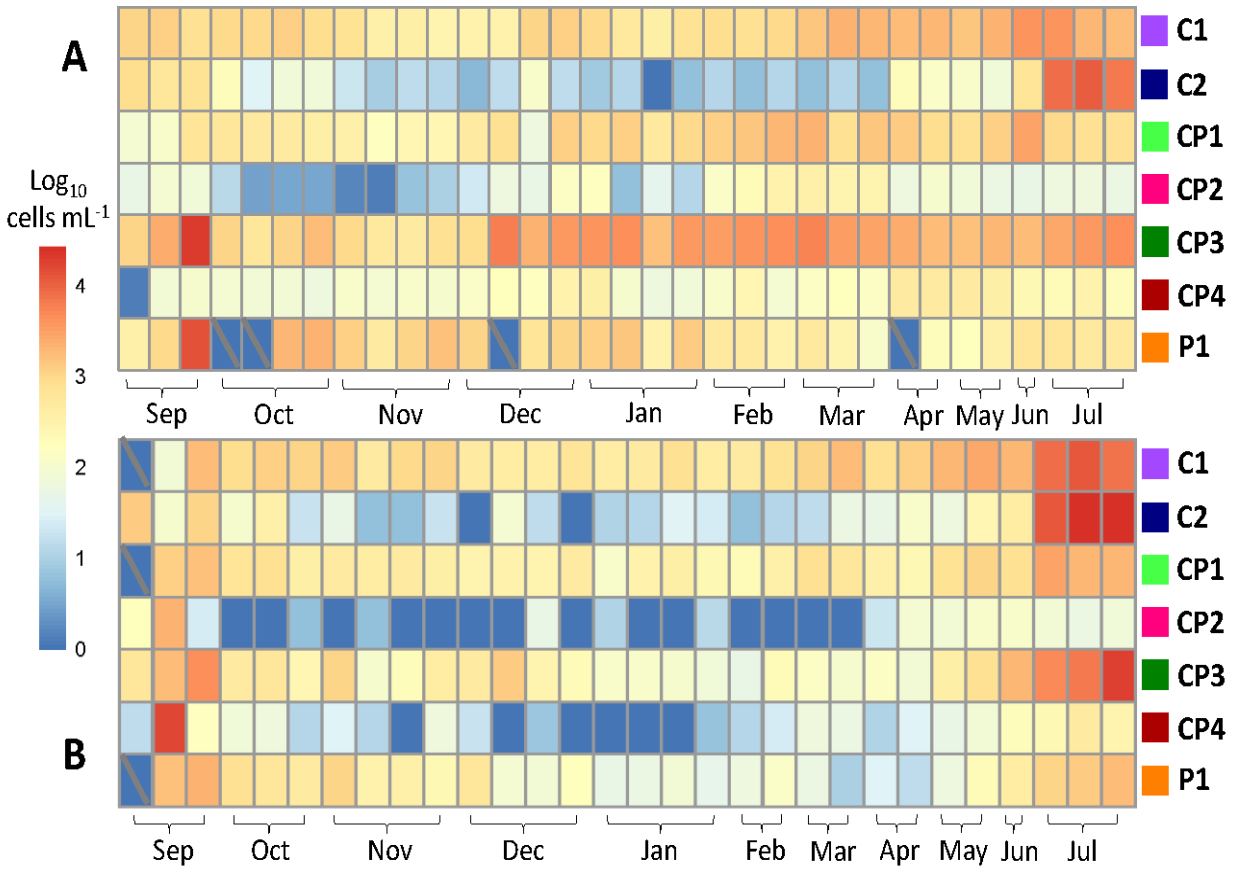

Figure 7. Heatmap displaying the log scale of population concentrations (cells per mL) in the Columbia (A) and Willamette (B) Rivers over the sampling timeframe. The color scale ranges from warm to cool colors representing high and low abundances, respectively. The 7 populations identified via flow cytometry are labeled on the right, colored as in Figure 3. Populations C1, CP1, and P1 each had days in either the Columbia or Willamette Rivers when their corresponding populations were not distinguishable and were thus marked with a grey slash.

Populations C1 and C2 were similar in that they both increased in abundance in the Columbia and Willamette Rivers as July approached. However, C2 abundances dropped more sharply than C1 during winter. CP1 abundances were steady throughout the sampling timeframe in both rivers, although I observed a slightly greater increase in abundance in spring for the Columbia and then in summer for the Willamette. CP2 was very low in abundance in both rivers in the late fall and winter months, but also increased in July. CP3 thrived in the Columbia during the winter and both rivers contained more of this population in September. CP4 was consistently abundant in the Columbia and much less abundant in the Willamette, especially during winter. And P1 had a greater abundance in the Columbia overall, with an increase in abundance in both rivers in September. Overall, the Columbia had a greater concentration of picophytoplankton over the sampling timeframe.

Environmental USGS data analysis

Environmental data was retrieved (Figure 8) from three USGS hydrological stations, two along the Columbia River and one along the Willamette River (see materials and methods Figure 2). All the hydrological data obtained from the Willamette River was less than one mile downriver at depths of around 6-18 feet. The hydrological conditions experienced by the surface populations studied are thus extrapolated between surface water sample and sensor depths. The discharge and turbidity data obtained from the Columbia River were also representative of the surface water samples with a similar sensor depth located approximately 1 mile downriver from the sample site. The temperature data, while not entirely representative of the sampling site

being close to 10 miles upriver, was still used as a proxy for how the water temperature changes downriver of the Bonneville Dam that eventually reaches the sampling site.

The environmental gradients followed a seasonal trend from September 2022 to July 2023 in both rivers. Specifically, discharge in cubic feet per second (cfs) increased for both rivers in winter and early spring and dropped as the summer approached (Figure 8A). Temperature (°C) decreased from fall to winter and increased from winter to summer with the Willamette River being slightly more variable in temperature (Figure 8C). The Willamette River was also more variable than the Columbia River in discharge and turbidity (Figure 8A,B). A greater number of peaks was observed in the Willamette River, with the largest turbidity peak of about 70 FNU around December 2022 (Figure 8B). The Columbia's largest turbidity peak was less than

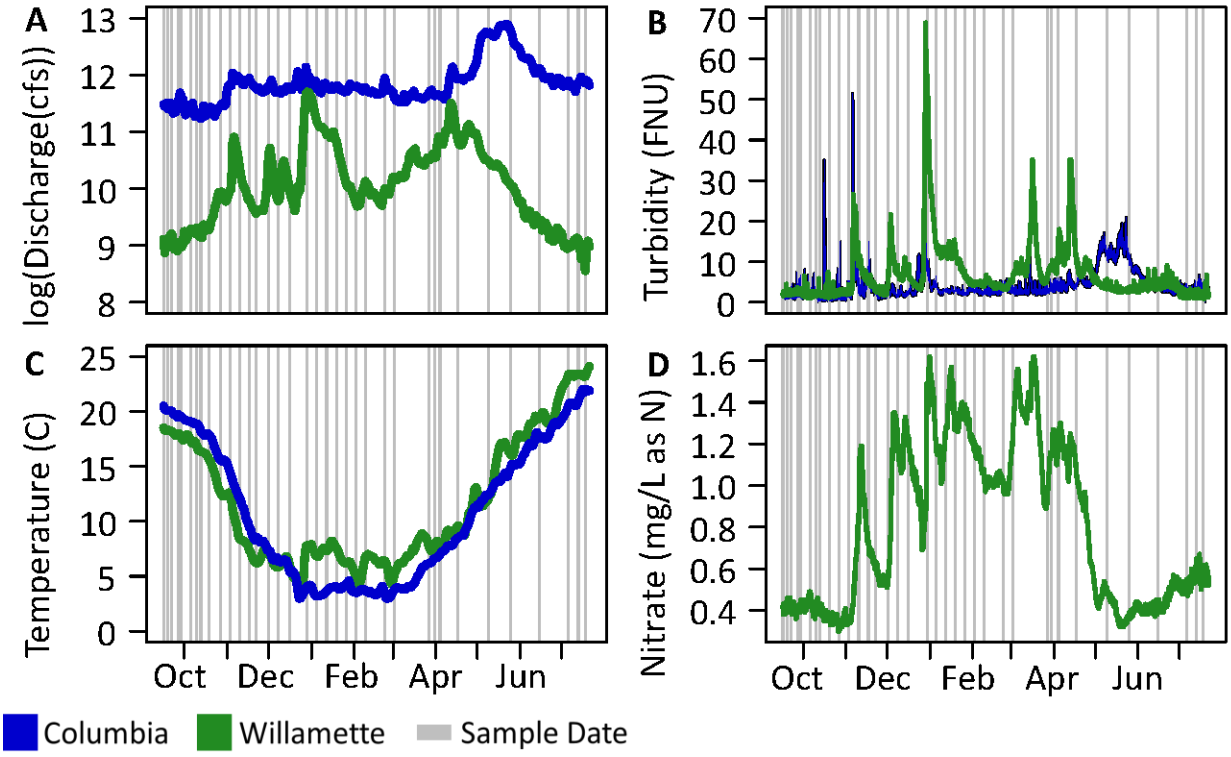

Figure 8. Environmental data obtained from USGS hydrological stations for the Columbia (blue) and Willamette (green) Rivers over the sampling timeframe. Grey vertical lines indicate the points samples were taken for flow cytometry A) Log scale of the daily average of discharge in cubic feet per second (cfs). B) Continuous readings of turbidity in Formazin Nephelometric Units (FNU). C) The daily average of temperature (°C). D) Continuous readings of nitrate in mg per L for the Willamette River only.

that of Willamette at around 50 FNU and occurred a bit earlier in November. Nitrate data, measured as mg per L of nitrogen, was only available for the Willamette River (Figure 8D). There was an inverse relationship between temperature and nitrate, with nitrate readings possibly contributing to some of the turbidity outputs (Figure 8B,C,D).

Technical reproducibility

To test the reproducibility of the flow cytometry method, I sampled repeatedly in both rivers at one timepoint on July 13, 2023. I found high reproducibility between technical replicates for the total particles, total chlorophyll positive cells, and totals for each population (Figure 9). There was a greater technical variability of cell concentrations in the Willamette River compared to the Columbia River recorded from that day due to one outlier. Furthermore, individual populations were technically variable in different ways. The least variable population in the Willamette was CP4 while the most variable population in the Willamette was P1. Population CP2 was quite variable in both the Columbia and Willamette. The rest of the Columbia River populations were much less variable with CP3 being the least so. The variability of the internal bead standards are not relevant in this case since I used them as a reference for laser alignment of forward light scatter and pigment fluorescence analysis and not as a means of calibrating for cell count. Flow rates were measured directly instead to assess the volumes of samples analyzed accounting for possible variability in concentration across analysis days.

Consistency of cell identities between samples was ensured via homogenous gating across all populations in all samples. Overlapping populations also occurred which were accounted for by deeming those as not gate-able and excluding those data points in the analysis

(Figure 9). The variability seen in the replicates taken from the Willamette River is not of major concern to the scope of the study based on the gradual differences in population abundances observed over time as compared to the variability recorded as the Willamette River was blooming. Further assessment of sampling technique variability should be considered in future studies.

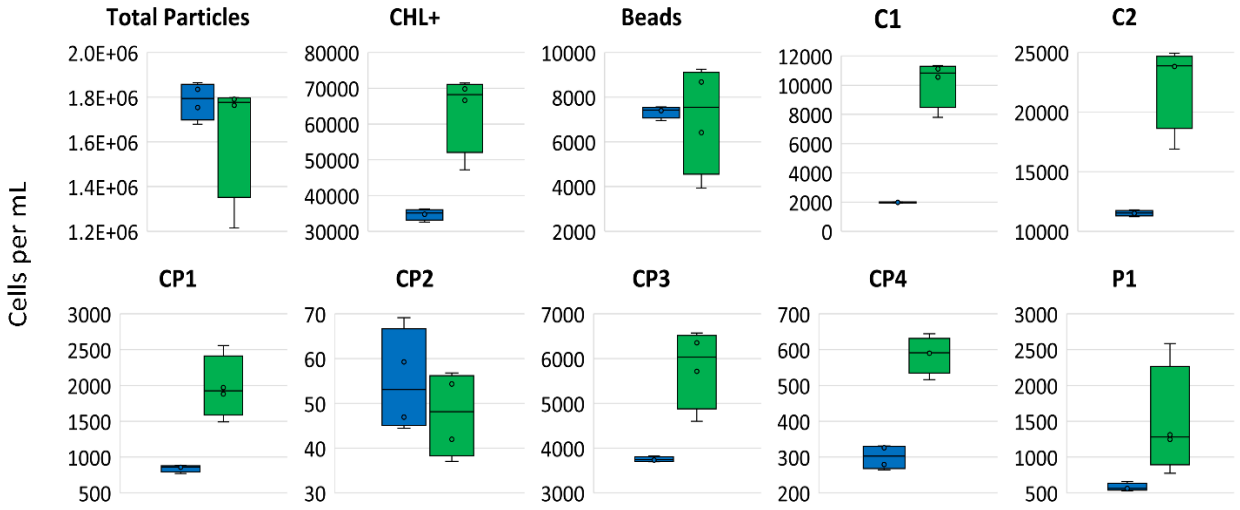

Figure 9. Box and whisker plots of each population's variability in the Columbia (blue) and Willamette (green) Rivers based on replicate samples taken within a 10m range along each sampling dock on July 13, 2023. The 'Total Particles' plot represents the samples before any FlowJo gating was applied. 'CHL+' represents the chlorophyll-containing cells within each sample. The 'Beads' in this plot are a mixture of 4.2 µm UltraRainbow and 1.0 µm Yellow Green beads within the same gate. The rest of the plots are labeled by population names seen previously. For boxplots, the middle line is the median with the top and bottom of the box representing the 75th and 25th percentile, respectively. The dots represent individual data points, with the whiskers representing the largest and smallest values.

Chapter 4

Discussion

To address the question of picophytoplankton ecology with respect to environmental conditions, I measured the abundance of the picophytoplankton communities in the Columbia and Willamette Rivers over a 10-month period. I identified seven populations that made up the overall picophytoplankton community. These were identified phenotypically via flow cytometric analysis of pigment fluorescences. While existence of phytoplankton (and presumptively picophytoplankton) in the Columbia and Willamette Rivers (Prahl et al., 1997; Small & Morgan, 1994; Sullivan, 1997; Sullivan et al., 2001) as well as from the Columbia estuary (Frame & Lessard, 2009; Haertel et al., 1969; Jones et al., 1990) has been studied, my work is the first to discover multiple subpopulations of the smallest phytoplankton existing in this system. In addition, my work shows that these populations have distinct phenotypes and that the two rivers are distinct in their seasonal cycles and community structures of the picophytoplankton populations. Tracking each picophytoplankton community over time suggests that there is niche partitioning between populations plus distinct dynamic ecological relationships within the Columbia and Willamette River ecosystems.

River picophytoplankton are composed of distinct populations that fill spectral niches

I identified seven distinct groups of picophytoplankton among the chlorophyll-containing cells in each river based on their unique pigment properties. Previous studies have shown that picocyanobacteria populations contain a range of smaller and larger cells, with the larger ones exhibiting greater amounts of fluorescence and similar fluorescence ratios to the smaller cells (Callieri, 2010; Gale et al., 2023), a phenomenon reflected in the “needles” (Thompson & Engh,

2016). In fact, those populations that are more needle-like in their distribution are likely to contain cells of varying size with the same fluorescence ratio, whereas those population distributions that are rounded are likely to contain cells of similar size with similar fluorescence ratios. One population, CP4, was unique in that it may have contained inconsistent subpopulations throughout the year based on inconsistent phycoerythrin fluorescence ratios between samples (Appendix D), so I did not attempt to discern between these subpopulations.

This identification of several phenotypic picophytoplankton populations indicates that these cells fill unique spectral niches in which they coexist by taking advantage of different wavelengths of sunlight via different pigmentations (Grébert et al., 2018, 2022). The parallel distributions of populations C1 and C2 on the relative chlorophyll fluorescence bivariate plots exemplifies their different chlorophyll pigment compositions. Similarly, CP2 and CP3 were parallel to CP4 and P1 which were parallel to CP1 on the bivariate chlorophyll fluorescence plots, demonstrating their different chlorophyll compositions (Appendix C). As for phycoerythrin compositions among the picophytoplankton, P1, CP3, and CP4 were parallel to CP1 and CP2 on the bivariate plots. Based on distribution locations on the two bivariate fluorescence plots, P1 and CP3 seemed most alike regarding pigment composition.

Inference of genotype based on phenotype

Phenotypic distinctions among the picophytoplankton may allude to genetic differences between populations. The congruence between phenotype and genotype has been shown for phytoplankton in other systems, such as the coastal ocean (Thompson & Engh, 2016) and large freshwater lakes (Gale et al., 2023). These populations likely consist of different types of prokaryotes and eukaryotes with different pigment signatures. Based on prior studies, I offer

hypotheses on the genetic identity of the different picophytoplankton populations in the Columbia and Willamette Rivers, which are organized in Table 1.

The large size, bright chlorophyll fluorescence, and lack of phycoerythrin of C1 and C2, suggested they may be picoeukaryotes. Other previous work in the Great Lakes has shown that a population of picophytoplankton only containing chlorophyll was identified as photosynthetic picoeukaryotes, likely Chlorophyta (green algae), a red-fluorescing organism (Fahnenstiel et al., 1991; Gale et al., 2023). Thus, it is most likely that populations C1 and C2, those that fit this previously established criteria, are a type of picoeukaryote. These picoeukaryote populations were of high abundance in both rivers likely due to their large genomes, which may support more versatile metabolism and greater adaptability. The other possible identity of these two populations is Type 1 *Synechococcus*, which have no phycoerythrin but do contain phycocyanin. Although I was unable to detect phycocyanin in this study, the smaller cells of C2 are more likely to be *Synechococcus* compared to the larger cells of C1.

I hypothesize that the populations CP1, CP2, CP3, and CP4 populations are from the Synechococcales lineage of picocyanobacteria, consisting of *Synechococcus* spp. and *Cyanobium* spp. Cells from these populations all contained both chlorophyll and phycoerythrin. These traits are typical of *Synechococcus* spp. of either Type II or Type III pigment composition, having phycocyanin and phycoerythrin I or having phycocyanin, phycoerythrin I, and phycoerythrin II, respectively (Gale et al., 2023); along with the possible identity of *Cyanobium* spp. being present (Cabello-Yves et al., 2022; Gale et al., 2023). To determine exactly which pigment types correspond to which population will require further analysis.

Our lab has also shown that some very small *Synechococcus* may exhibit less well-defined chlorophyll needles due to the limit of detection for chlorophyll emission on small cells; since it's been previously observed that some picocyanobacteria species can acclimate to high light levels of surface waters, resulting in less emission (Thompson & Engh, 2016). This makes *Synechococcu*s spp. of pigment type 2 or 3 the most likely classification for P1 since it contains both pigments with a less-defined chlorophyll distribution.

Table 1. Hypothesized genetic classifications of phenotypic picophytoplankton populations.

Phenotypic populations	**Hypothesized genetic classifications**
C1	Chlorophyta or pigment type 1 *Synechococcus* sp.
C2	Chlorophyta or pigment type 1 *Synechococcus* sp.
CP1	pigment type 2/type 3 *Synechococcus* sp. or *Cyanobium* sp.
CP2	pigment type 2/type 3 *Synechococcus* sp. or *Cyanobium* sp.
CP3	pigment type 2/type 3 *Synechococcus* sp. or *Cyanobium* sp.
CP4	pigment type 2/type 3 *Synechococcus* sp. or *Cyanobium* sp.
P1	pigment type 2/type 3 *Synechococcus* sp.

This phenotypic and genetic diversity among the picophytoplankton of the Columbia and Willamette Rivers suggests that they take advantage of different wavelengths of sunlight to coexist among each other. This phenomenon called "spectral niche partitioning" (Grébert et al., 2018, 2022), is well known in the open ocean and large lakes, but is not studied in rivers. Spectral properties of phytoplankton have been shown to vary in comparison to changes in genetic diversity, and environmental parameters like nutrient levels (Behrenfeld & Milligan, 2013; Scanlan & West, 2002; Six et al., 2007). The extent of biodiversity among the prokaryotic and eukaryotic picophytoplankton populations may also be linked to trophic interactions in the

aquatic ecosystem with some predators preferring different sizes of microbial prey cells (Callieri et al., 2012, 2016).

Large size ranges allude to microcolony formation

Five of the populations I identified contained cells that spanned a wide range of sizes. The wide ranges of cell size are reminiscent of microcolony formation in freshwater Synechococcales (Callieri et al., 2012, 2016; Jezberová & Komárková, 2007). Specifically, the bimodal size distributions of C2 and CP2 suggest that these populations are the most likely to form microcolonies. Thus, my data shows that microcolony formation is likely a relevant physiological state of these cells in river systems. Previous work shows that microcolony formation is used as a defense mechanism by providing a safe place for individual cells from predators or creating a particle too large for predation and is used to assist with chemical signaling between cells (Corno et al., 2013; Hence et al., 2007; Jezberová & Komárková, 2007; Müller et al., 2006). In addition, microcolony formation specifically of *Synechococcus* spp. rich in phycoerythrin has been suggested to be a defense strategy against UV radiation as well for those cells that lack protective pigments (Callieri et al., 2011).

Microcolony formations in the Columbia and Willamette Rivers are likely formed based on previously stated defense strategies like protection against predation or UV radiation for PE-rich cells specifically (Callieri et al., 2011; Corno et al., 2013; Hence et al., 2007; Jezberová & Komárková, 2007; Müller et al., 2006). The experimental system I developed involving seasonal coverage of surface water samples, precise single-cell measurements, and environmental data retrieval can be used as a platform to further investigate why photosynthetic cells form microcolonies and how this physiology responds to environmental conditions.

Picophytoplankton seasonal abundance

Picophytoplankton populations within each river had distinct patterns of abundance. These different patterns suggest that the microbial ecosystem of the two rivers is different though the sampling sites experience the same regional environmental conditions. This phenomenon mirrors the estimation of marine *Synechococcus* blooms being the most and least abundant in March and July, respectively (Flombaum et al., 2013), since the peaks and valleys of picophytoplankton concentrations in the Columbia and Willamette Rivers did not follow this pattern. Instead, blooms in the Columbia and Willamette Rivers were in fall and summer, not spring, with the Willamette having an additional small winter bloom. Plus, times of relatively lower picophytoplankton concentration spanned from October to March, not July. Additionally, these peaks and valleys of picophytoplankton concentrations were composed of different populations blooming at different time points.

Hydrological conditions controlled by dams

This thesis suggests that the flowing freshwater ecosystems of the Columbia and Willamette Rivers could be considered a unique natural laboratory for studying picophytoplankton in rivers. Results showed that picophytoplankton communities were more abundant in the Columbia than the Willamette over the entire period. One explanation is that the Columbia River is unique in the multitude of dams that form a series of elongated reservoirs (Harden, 1996). These slower flowing sections of water in the Columbia River has led to what's known as a "green" river system based on the well-known abundance of phytoplankton thriving in the relatively stagnant waters (Sullivan et al., 2001).

This immense growth of phytoplankton in the Columbia River may be due to the slower flow behind dams that allows sediment to settle, which leads to less turbidity and therefore more available sunlight. This phenomenon is reflected in the turbidity data showing less peaks in the Columbia River versus the Willamette River. Dam operation can also lead to a lag in seasonal temperature shifts since high volumes of water are released at controlled times (Sun et al., 2021). This reasoning, along with the greater volume of the Columbia River, can help explain why its temperature ended up cooler than the Willamette River over winter and took longer to increase in temperature from spring to summer.

In contrast to the many dams along the Columbia River, the only dams present in the Willamette River basin are along some tributaries, but not directly on the Willamette River (Nagel, 2017). This makes the Willamette River's dynamics based on natural phenomena like rainfall, helping to explain why the Willamette River had more events of turbidity (Sullivan, 1997). These turbidity events may also be linked to the greater variability of discharge observed in the Willamette River, resulting in more frequent mixing, thus upwelling of sediment (Chen & Chang, 2019). So, it seems that greater turbidity levels in the Willamette River led to less available sunlight for aquatic organisms to harvest in this system, resulting in a lower abundance of picophytoplankton due to the suspended particles (e.g., sediment) blocking and diffracting rays of sunlight.

Ecological relationships

Picocyanobacteria, especially those of Synechococcales, have been shown to demonstrate extreme plasticity with their prevailed abundance through various temperatures and light levels combined with their ability to form microcolonies to relieve environmental stress

(Callieri, 2017). My time series of surface water samples from the Columbia and Willamette Rivers showed that most of the picophytoplankton communities increased and decreased in abundance according to temperature shifts. In general, the population abundance patterns seemed to mimic seasonal changes by decreasing from fall to winter, and increasing from spring to summer, as temperature decreased and increased, respectively.

An oceanic model by Flombaum et al. (2013) showed that increases in global temperatures will lead to a significant increase in overall phytoplankton abundance. Predicted maximum abundance of *Synechococcus* in our oceans was at 10 °C (Flombaum et al., 2013). Similarly, P1, a likely *Synechococcus* sp., relatively increased in abundance between November to December in the Columbia River, when the temperature was around 10 °C. Populations CP3 relatively increased in both rivers around this time but increased more dramatically in the Columbia River in comparison to the Willamette River by December. From April to May, when the temperature of each river was around 10 °C once more, all picophytoplankton populations except for CP2 in the Columbia River began to increase in abundance. So, it seems that P1 of the Columbia River and CP3 of both rivers reflected the growth vs. temperature relationship of marine *Synechococcus spp.*, while the rest of the populations, except for Columbia's CP2, partially reflected this relationship.

In contrast to the previous model predicting a maximum abundance of *Synechococcus* at 10 °C, a study of Lake Maggiore by Callieri & Piscia (2002) showed that freshwater picophytoplankton were maximally abundant around 18-20 °C. These temperatures occurred in the Columbia and Willamette Rivers from September to October and from June to July, being before and after the 10 °C state discussed previously. Picophytoplankton populations of the

Columbia River that increased relatively in abundance in September to October were C1, CP1, CP3, and P1; and those that increased relatively from June to July were C1, C2, CP3, and P1. So, C1, CP3, and P1 in the Columbia River most follow the relationship of freshwater picophytoplankton growth vs. temperature, with CP1 and C2 having somewhat of a similar relationship. Overall, the Columbia seemed to support picophytoplankton growth dynamically throughout the year.

At the same time, all the picophytoplankton populations of the Willamette River began decreasing from September to October, with most peaking in abundance at the end of September. However, from June to July, all except for CP2 in the Willamette River increased relatively in abundance. This suggests that the conditions in the Willamette River favor picophytoplankton growth in the early fall and mid-summer which follows suit of previously observed increases in phytoplankton growth due to increases in temperature (Beardall & Raven, 2004).

Interestingly, CP2 had its own unique abundance pattern in both rivers. In the Columbia River, CP2 was the most abundant from February to March, a time of cooler temperatures and relatively less daylight than most of the year. The increased abundance of CP2 during these months might help explain how the optimum growth rate for some *Synechococcus* has been shown to occur at lower light intensities (Morris & Glover, 1981; Gervais et al., 1997; Glover et al., 1985), which would also explain the abundance pattern of CP1 in the Columbia. This does not mean however, that Synechococcales that prefer warmer temperatures do not prefer lower light levels because CP3 of the Columbia River adjusted to both cold/dark and warm/lighter seasons of the Columbia River, blooming from December to July. In comparison, the abundance of CP2 in

the Willamette River increased in September and May, thus bloomed in fall and spring, however the environmental conditions supporting the two blooms remain unclear.

Furthermore, phytoplankton growth in the fall has been shown to rely on the balance between decreasing light availability and increasing nutrient availability (Longhurst, 2007). In the Northwest Pacific Ocean, fixed nitrogen is typically the limiting factor for primary production (Hashihama et al., 2009; Li, Q., et al., 2015; Longhurst, 2007; Moore, C. M., et al., 2013; Moore, J. K., et al., 2004). Yet, freshwater phytoplankton strains seem to cope with varying levels of nitrogen using additional copies of a global nitrogen regulator as well as glutamine synthetases, with only one strain of freshwater picocyanobacteria reported to fix nitrogen (via nitrogenase) (Cabello-Yeves et al., 2022; Di Cesare et al., 2018). The Willamette River reflected the balance of nutrients and light availability by having an inverse relationship between temperature and nitrate over the period. This relationship could explain the slight abundance peaks of CP3 in the Willamette River throughout the winter season, meaning that CP3 may be able to adapt to lower light/temperature conditions by taking advantage of more available nutrients, like nitrate. On the other hand, C2 and CP2 had very low abundances in the winter months for both rivers, which suggests that these populations require more sunlight and less nutrients.

Future directions

The time-series I conducted sets the foundation to address many more questions on the ecology of picophytoplankton and their relationships to environmental dynamics and change. My next steps include applying a Mie theory calibration to acquire predicted diameter (instead of relative size), plus statistical and genetic analyses to link phenotypes to genotypes.

The relationship between forward light scatter detected and the size of events (i.e., beads and cells) could be further teased out using a range of fluorescent particles of different sizes to fully calibrate the flow cytometer according to the analysis performed in this study (Ribalet et al., 2019).

The statistical analysis will involve Non-metric Multidimensional Scaling (NMDS) to calculate correlations between changes in population abundances and hydrological parameters. Environmental data other than the parameters investigated here should also be of interest to those who wish to conduct a similar study. For example, measurements of sulfur may be useful in ecological analysis since freshwater strains have proven to be better adapted to sulfur uptake (Cabello-Yeves et al., 2022).

Genetic analysis will be the next step to connect the phenotypic populations to their genotypes. Phylogenetic analysis of the *Synechococcus* spp. 16S rRNA gene has shown that there is extensive ecosystem-specific diversity among *Synechococcus* with closely related species thriving in similar but distant ecosystems throughout the globe (Crosbie et al., 2003; Ernst et al., 2003; Scanlan & West, 2002). Additionally, retention of horizontally transferred genes based on nutritional or bioenergetic pressures may have resulted in niches for a variety of cells with specialized metabolisms (Falkowski et al., 2008). Ecological niches thus correspond to light and nutrient availability, all of which are vital to modeling biogeochemical freshwater systems (Ahlgren & Rocap, 2006; Scanlan & West, 2002; Stomp et al., 2004, 2007). This work emphasizes the importance of the phenotypic analysis conducted while acknowledging the need to connect these findings to the microbiome.

Those who would like to continue this type of sampling scheme in the future should consider even more frequent sampling. A higher sampling resolution could provide more detailed changes in picophytoplankton abundance along with greater assurance in extreme fluctuations. The technical reproducibility was assessed using various samples within a 10-meter range of the sampling site at a single time point. While this analysis resulted in a greater variability of population concentrations detected in the Willamette, compared to the Columbia, it's not easy to apply this variability to every sample based on dynamic hydrological conditions throughout the year. With that, performing multiple daily samples might provide insight into weekly versus daily variability of picophytoplankton abundance in the rivers. Further work could also investigate increased disturbance effects, such as more frequent heat waves or river pollution.

Conclusion

I investigated the abundance, diversity, and hypothesized function of resident picophytoplankton populations of the Columbia and Willamette Rivers. The research questions are addressed as follows: (1) I first wanted to know how many different phenotypic picophytoplankton populations were in each river. This question was answered using a hierarchal flow cytometry gating scheme on cells of like pigment fluorescence. Results showed that there were seven distinct populations present in each river. The populations between the two rivers were named the same due to having similar fluorescence ratios. (2) Next, I was curious as to how the population concentrations might shift over time and how these shifts compared between the two rivers. Through data analysis, each population had its own unique seasonal abundance pattern, with some similar trends observed between populations across the two ecosystems. (3) Finally, I wanted to determine if differences in picophytoplankton abundances between the

Columbia and Willamette Rivers were based on differences observed between the two environments. Significant differences in the physical habitat of each system provided unique hydrological conditions for picophytoplankton communities, somewhat corresponding to the observed abundance patterns.

These findings are the first major step in understanding the biogeochemical relationship between picophytoplankton communities and the natural laboratory of Portland, Oregon's major river systems. Further work will focus on the genetic identification of these phenotypically distinct cells plus the statistical correlation of population abundance fluctuations with environmental changes. Efforts made to understand this system will be useful in illuminating which picophytoplankton populations most drive energy and nutrient cycles in the Columbia and Willamette Rivers.

References

Ahlgren, N. A. & Rocap, G. (2006, November 1). Culture Isolation and Culture-Independent Clone Libraries Reveal New Marine Synechococcus Ecotypes with Distinctive Light and N Physiologies. *Applied and Environmental Microbiology, 72*, 7193-7204. https://doi.org/10.1128/AEM.00358-06

Beardall, J., & Raven, J. A. (2004). The potential effects of global change on microalgal photosynthesis, growth and ecology. *Phycologia*, *43*(1), 26-40. https://doi.org/10.2216/i0031-8884-43-1-26.1

Behrenfeld, M. J., & Milligan, A. (2013, January). Photophysiological expressions of iron stress in phytoplankton. *Annual Review of Marine Science, 5*, 217–246. https://doi.org/10.1146/annurev-marine-121211-172356

Biller, S. J., Berube, P. M., Lindell, D., & Chisholm, S. W. (2015). *Prochlorococcus*: the structure and function of collective diversity. *Nature Reviews Microbiology, 13*, 13–27. https://doi.org/10.1038/nrmicro3378

Bongard, J. (2018, June 13). How Streamflow is Measured. *U. S. Geological Survey Water Science School.* https://www.usgs.gov/special-topics/water-science-school/science/how-streamflow-measured#overview

Buitenhuis, E. T., Pangerc, T., Franklin, D. J., Le Quere, C., & Malin, G. (2008, May 21). Growth rates of six coccolithophorid strains as a function of temperature. *Limnology and Oceanography, 53*(3), 1181–1185. https://doi.org/10.4319/lo.2008.53.3.1181

Cabello-Yeves, P. J., Callieri, C., Picazo, A., Schallenberg, L., Huber, P., Roda-Garcia, J. J., Bartosiewicz, M., Belykh, O. I., Tikhonova, I. V., Torcello-Requena, A., De Prado, P. M., Puxty, R. J., Millard, A. D., Camacho, A., Rodriguez-Valera, F., & Scanlan, D. J. (2022). Elucidating the picocyanobacteria salinity divide through ecogenomics of new freshwater isolates. *BMC Biology*, *20*(1), 175. https://doi.org/10.1186/s12915-022-01379-z

Callieri, C., Amicucci, E., Bertoni, R., & Vörös, L. (1996). Fluorometric Characterization of Two Picocyanobacteria Strains from Lakes of Different Underwater Light Quality. *International Review of Hydrobiology, 81*(1), 13-23. https://doi.org/10.1002/iroh.19960810103

Callieri, C. & Piscia, R. (2002). Photosynthetic efficiency and seasonality of autotrophic picoplankton in Lago Maggiore after its recovery. *Freshwater Biology 47*, 941-956.

Callieri, C. (2008, March 1). Picophytoplankton in Freshwater Ecosystems: The Importance of Small-Sized Phototrophs. *Freshwater Reviews, 1*(1), 1-28. https://doi.org/10.1608/FRJ-1.1.1

Callieri, C. (2010). Single cells and microcolonies of freshwater picocyanobacteria: A common ecology. *Journal of Limnology*, *69*(2), 257. https://doi.org/10.4081/jlimnol.2010.257

Callieri, C., Lami, A., & Bertoni, R. (2011, November). Microcolony Formation by Single-Cell Synechococcus Strains as a Fast Response to UV Radiation. *Applied and Environmental Microbiology, 77*(21), 7533–754. https://doi.org/10.1128/AEM.05392-11

Callieri, C., Cronberg, G., & Stockner, J. G. (2012, January 1). Freshwater Picocyanobacteria: Single Cells, Microcolonies and Colonial Forms. In Ecology of Cyanobacteria II, Whitton, B. A. (ed). New York, NY*: Springer,* 229–269. http://dx.doi.org/10.4081/jlimnol.2010.257

Callieri, C., Amalfitano, S., Corno, G., & Bertoni, R. (2016, November 11). Grazing-induced *Synechococcus* microcolony formation: experimental insights from two freshwater phylotypes. *FEMS Microbiology Ecology, 92*(11), fiw154. https://doi.org/10.1093/femsec/fiw154

Callieri, C. (2017). Synechococcus plasticity under environmental changes. *FEMS Microbiology Letters*, *364*(23). https://doi.org/10.1093/femsle/fnx229

Camacho, A., Picazo, A., Miracle, M. R., & Vicente E. (2003, August). Spatial distribution and temporal dynamics of picocyanobacteria in a meromictic karstic lake. *Algological Studies 109 = Arch. Hydrobiol. Suppl., 109*, 171–184. http://dx.doi.org/10.1127/1864-1318/2003/0109-0171

Chen, J., & Chang, H. (2019). Dynamics of wet-season turbidity in relation to precipitation, discharge, and land cover in three urbanizing watersheds, Oregon. *River Res Applic*., *35*, 892–904. https://doi.org/10.1002/rra.3487

Chisholm, S. W. (1992). Phytoplankton Size. In: Falkowski, P.G., Woodhead, A.D., Vivirito, K. (eds) Primary Productivity and Biogeochemical Cycles in the Sea. *Environmental Science Research, 43,* 213-237. Springer, Boston, MA. https://doi.org/10.1007/978-1-4899-0762-2_12

Christoffersen, K. (1994). Variation of feeding activities of heterotrophic nanoflagellates on picoplankton. *Mar. Microb. Food Web, 8*, 11-123. http://pascal-francis.inist.fr/vibad/index.php?action=getRecordDetail&idt=3329795

Corno, G., Villiger, J., & Pernthaler, J. (2013, April). Coaggregation in a microbial predator-prey system affects competition and trophic transfer efficiency. *Ecology, 94*(4), 870–881. http://www.jstor.org/stable/23436300

Crosbie, N. D., Pöckl, M., & Weisse, T. (2003, September). Dispersal and phylogenetic diversity of nonmarine picocyanobacteria, inferred from 16S rRNA gene and cpcBA-intergenic spacer sequence analyses. *Applied and Environmental Microbiology, 69*(9), 5716-5721. https://doi.org/10.1128/AEM.69.9.5716-5721.2003

De Cicco, L. A., Hirsch, R. M., Lorenz, D., Watkins, W. D., & Johnson, M. (2023). dataRetrieval: R packages for discovering and retrieving water data available from Federal hydrologic web services, *R package version 2.7.13*. https://code.usgs.gov/water/dataRetrieval

Di Cesare, A., Cabello-Yeves, P. J., Chrismas, N. A. M., Sánchez-Baracaldo, P., Salcher, M. M., & Callieri, C. (2018). Genome analysis of the freshwater planktonic *Vulcanococcus limneticus* sp. nov. reveals horizontal transfer of nitrogenase operon and alternative pathways of nitrogen utilization. *BMC Genomics, 19*, article no. 259. https://doi.org/10.1186/s12864-018-4648-3

Dutkiewicz, S., Morris, J. J., Follows, M. J., Scott, J., Levitan, O., Dyhrman, S. T., & Berman-Frank, I. (2015, July 20). Impact of ocean acidification on the structure of future phytoplankton communities. *Nature Climate Change, 5*, 1002–1006. https://doi.org/10.1038/nclimate2722

Dutkiewicz, S., Boyd, P. W., & Riebesell, U. (2021). Exploring biogeochemical and ecological redundancy in phytoplankton communities in the global ocean. *Global Change Biology*, *27*(6), 1196–1213. https://doi.org/10.1111/gcb.15493

Engh, G. van den, & Stokdijk, W. (1989). Parallel processing data acquisition system for multilaser flow cytometry and cell sorting. *Cytometry*, *10*(3), 282–293. https://doi.org/10.1002/cyto.990100307

Ernst, A. (1991). Cyanobacterial picoplankton from Lake Constance I. Isolation by fluorescence characteristics. *Journal of Plankton Research, 13*(6), 1307-1312. https://doi.org/10.1093/plankt/13.6.1307

Ernst, A., Becker, S., Wollenzien, U. I. A., & Postius, C. (2003, January). Ecosystem dependent adaptive radiations of picocyanobacteria inferred from 16S rRNA and ITS-1 sequence analysis. *Microbiology (Reading), 149*(1), 217–228. https://doi.org/10.1099/mic.0.25475-0

Everroad, R. C., & Wood, A. M. (2006, November 16). Comparative molecular evolution of newly discovered picocyanobacterial strains reveals a phylogenetically informative variable region of beta-phycoerythrin. *Journal of Phycology, 42*(6), 1300-1311. https://doi.org/10.1111/j.1529-8817.2006.00282.x

Falkowski P. G., & Raven, J. A. (2000, December). Aquatic Photosynthesis*. International Microbiology, 3*(4), 259-265. https://www.researchgate.net/publication/41931921_Aquatic_Photosynthesis_Paul_G_Falkowski_John_A_Raven#fullTextFileContent

Falkowski, P. G., Fenchel, T., & Delong, E. F. (2008). The Microbial Engines That Drive Earth's Biogeochemical Cycles. *Science*, *320*(5879), 1034–1039. https://doi.org/10.1126/science.1153213

Falkowski, P. G., & Godfrey, L. V. (2008). Electrons, life and the evolution of Earth's oxygen cycle. *Philosophical Transactions of the Royal Society B: Biological Sciences*. https://doi.org/10.1098/rstb.2008.0054

Fahnenstiel, G. L., Carrick, H. J., Rogers, C. E., & Sicko-Goad, L. (1991). Red Fluorescing Phototrophic Picoplankton in the Laurentian Great Lakes: What Are They and What Are They Doing? *International Review of Hydrobiology, 76*(4), 603-616. https://doi.org/10.1002/iroh.19910760411

Field, C. B., Behrenfeld, M. J., Randerson, J. T., & Falkowski, P. (1998). Primary Production of the Biosphere: Integrating Terrestrial and Oceanic Components. *Science*, *281*(5374), 237–240. https://doi.org/10.1126/science.281.5374.237

Flombaum, P., Gallegos, J.L., Gordillo, R.A., Rincón, J., Zabala, L. L., Jiao, N., Karl, D. M., Li, W. K. W., Lomas, M. W., Veneziano, D., Vera, C. S., Vrugt, J. A., & Martiny, A. C. (2013). Present and future global distributions of the marine Cyanobacteria Prochlorococcus and Synechococcus. *PNAS*, *110*(24). https://doi.org/10.1073/pnas.1307701110

Frame, E. R., & Lessard, E. J. (2009). Does the Columbia River plume influence phytoplankton community structure along the Washington and Oregon coasts? *Journal of Geophysical Research: Oceans*, *114*(C2). https://doi.org/10.1029/2008JC004999

Gale, J., Sweeney, C., Paver, S., Coleman, M. L., & Thompson, A. W. (2023, September 4). Diverse and variable community structure of picophytoplankton across the Laurentian Great Lakes. *Limnology and Oceanography*. https://doi.org/10.1002/lno.12422

Gervais, F., Padisák, J., & Koschel, R. (1997, June). Do light quality and low nutrient concentration favour picocyanobacteria below the thermocline of the oligotrophic Lake Stechlin? *Journal of Plankton Research, 19*(6), 771- 781. https://doi.org/10.1093/plankt/19.6.771

Glover, H. E., Phinney, D. A., & Yentsch, C. S. (1985). Photosynthetic Characteristics of Picoplankton Compared with Those of Larger Phytoplankton Populations, in Various Water Masses in the Gulf of Maine. *Biological Oceanography, 3*(3), 223-248. https://www.tandfonline.com/doi/pdf/10.1080/01965581.1985.10749474

Grébert, T., Doré, H., Partensky, F., Farrant, G. K., Boss, E. S., Picheral, M., Guidi, L., Pesant, S., Scanlan, D. J., Wincker, P., Acinas, S. G., Kehoe, D. M., & Garczarek, L. (2018). Light color acclimation is a key process in the global ocean distribution of Synechococcus cyanobacteria. *PNAS, 115*(9), E2010–E2019. https://doi.org/10.1073/pnas.1717069115

Grébert, T., Garczarek, L., Daubin, V., Humily, F., Marie, D., Ratin, M., Devailly, A., Farrant, G. K., Mary, I., Mella-Flores, D., Tanguy, G., Labadie, K., Wincker, P., Kehoe, D. M., & Partensky, F. (2022). Diversity and Evolution of Pigment Types in Marine Synechococcus Cyanobacteria. *Genome Biology and Evolution, 14*(4). https://doi.org/10.1093/gbe/evac035

Haertel, L., Osterberg, C., Curl, H., & Park, P. K. (1969). Nutrient and Plankton Ecology of the Columbia River Estuary. *Ecology*, *50*(6), 962–978. https://doi.org/10.2307/1936889

Harden, B. (1996). A river lost: the life and death of the Columbia. *New York, W.W. Norton.*

Hashihama, F., Furuya, K., Kitajima, S., Takeda, S., Takemura, T., & Kanda, J. (2009, February 13). Macro-scale exhaustion of surface phosphate by dinitrogen fixation in the western North Pacific. *Geophysical Research Letters, 36*(3). https://doi.org/10.1029/2008GL036866

Haverkamp, T. H. A., Schouten, D., Doeleman, M., Wollenzien, U., Huisman, J., & Stal, L. J. (2009). Colorful microdiversity of Synechococcus strains (picocyanobacteria) isolated from the Baltic Sea. *The ISME Journal, 3*(4), Article 4. https://doi.org/10.1038/ismej.2008.118

Hence, B. A., Kuttler, C., Müller, J., Rothballer, M., Hartmann, A., & Kreft, J. (2007, March). Does efficiency sensing unify diffusion and quorum sensing? *Nature Reviews Microbiology, 5*, 230-239. https://doi.org/10.1038/nrmicro1600

IPCC. (2001). 2001: Climate Change 2001: The Scientific Basis. Contribution of Working Group I to the Third Assessment Report of the Intergovernmental Panel on Climate Change [Houghton, J.T., Y. Ding, D.J. Griggs, M. Noguer, P.J. van der Linden, X. Dai, K. Maskell, and C.A. Johnson (eds.)]. *Cambridge University Press,* Cambridge, United Kingdom and New York, NY, USA. https://www.ipcc.ch/site/assets/uploads/2018/03/WGI_TAR_full_report.pdf

Jezberová, J., & Komárková, J. (2007, July). Morphological transformation in a freshwater Cyanobium sp. induced by grazers. *Environmental Microbiology, 9*(7), 1858–1862. https://doi.org/10.1111/j.1462-2920.2007.01311.x

Jones, K. K., Simenstad, C. A., Higley, D. L., & Bottom, D. L. (1990). Community structure, distribution, and standing stock of benthos, epibenthos, and plankton in the Columbia River Estuary. *Progress in Oceanography*, *25*(1–4), 211–241. https://doi.org/10.1016/0079-6611(90)90008-P

Kluyver, A. J., & Donker, H. J. (1926). Die Einheit in der Biochemie. *Borntraeger*.

Koch, C., Günther, S., Desta, A. F., Hübschmann, T., & Müller, S. (2013, January 3). Cytometric fingerprinting for analyzing microbial intracommunity structure variation and identifying subcommunity function. *Nature Protocols, 8*, 190–202. https://doi.org/10.1038/nprot.2012.149

Kolde, R. (2019). _pheatmap: Pretty Heatmaps_. *R package version 1.0.12*. https://CRAN.R-project.org/package=pheatmap

Lewandowska, A. M., Breithaupt, P., Hillebrand, H., Hoppe, H. G., Jürgens, K., & Sommer, U. (2012). Responses of primary productivity to increased temperature and phytoplankton diversity. *Journal of Sea Research*, *72*, 87-93.

Li, Q., Legendre, L., & Jiao, N. (2015, February 27). Phytoplankton responses to nitrogen and iron limitation in the tropical and subtropical Pacific Ocean. *Journal of Plankton Research, 37*(2), 306– 319. https://doi.org/10.1093/plankt/fbv008

Li, W. K. W. (2003, December 22). Annual average abundance of heterotrophic bacteria and Synechococcus in surface ocean waters. *Limnology and Oceanography, 43*(7), 1743-1753. https://doi.org/10.4319/lo.1998.43.7.1746

Litchman, E., de Tezanos Pinto, P., Edwards, K. F., Klausmeier, C. A., Kremer, C. T., & Thomas, M. K. (2015). Global biogeochemical impacts of phytoplankton: A trait-based perspective. *Journal of Ecology*, *103*(6), 1384–1396. https://doi.org/10.1111/1365-2745.12438

Longhurst, A. R. (2007, January 1). Ecological Geography of the Sea. *Elsevier*. http://dx.doi.org/10.1016/B978-0-12-455521-1.X5000-1

Moreria-Turcq, P., Martin, J. M., & Fleury, A. (1993, July). Chemical and biological characterization of particles by flow cytometry in the Krka estuary, Croatia. *Marine Chemistry, 43(*1-4), 115-126. https://doi.org/10.1016/0304-4203(93)90219-E

Moore, J. K., Doney, S. C., & Lindsay, K. (2004, December 14). Upper ocean ecosystem dynamics and iron cycling in a global three-dimensional model. *Global Biogeochemical Cycles, 18*(4). https://doi.org/10.1029/2004GB002220

Moore, C. M., Mills, M. M., Arrigo, K. R., Berman-Frank, I., Bopp, L., Boyd, P. W., Galbraith, E. D., Geider, R. J., Guieu, C., Jaccard, S. L., Jickells, T. D., La Roche, J., Lenton, T. M., Mahowald, N. M., Marañón, E., Marinov, I., Moore, J. K., Nakatsuka, T., Oschlies, A., Saito, M. A., Thingstad, T. F., Tsuda, A., & Ulloa, O. (2013, March 31). Processes and patterns of oceanic nutrient limitation. *Nature Geoscience, 6*, 701–710. https://doi.org/10.1038/ngeo1765

Morris, I., & Glover, H. E. (1981, September). Physiology of photosynthesis by marine coccoid cyanobacteria--Some ecological implications. *Limnology and Oceanography, 26*(5), 957-961. https://doi.org/10.4319/lo.1981.26.5.0957

Müller, J., Kuttler, C., Hence, B. A., Rothballer, M., & Hartmann, A. (2006, October). Cell-cell communication by quorum sensing and dimension-reduction. *Journal of Mathematical Biology, 53*(4), 672–702. https://doi.org/10.1007/s00285-006-0024-z

Nagel, A. C. (2017). Analyzing Dam Feasibility in the Willamette River Watershed. *Dissertations and Theses, PDXScholar,* Paper 4012. https://doi.org/10.15760/etd.5896

Nelson, D., Cox, M., & Hoskins, A. (2021). Lehninger: Principles of Biochemistry. *W.H. Freeman and Company*, *8*, 700-740.

Nolan, M. (2018, June 6). Turbidity and Water. *U. S. Geological Survey Water Science School*. https://www.usgs.gov/special-topics/water-science-school/science/turbidity-and-water#overview

Olson, R. J., Frankel, S. L., Chisholm, S. W., & Shapiro, H. M. (1983, April 8). An inexpensive flow cytometer for the analysis of fluorescence signals in phytoplankton: Chlorophyll and DNA distributions. *Journal of Experimental Marine Biology and Ecology, 68*(2), 129-144. https://doi.org/10.1016/0022-0981(83)90155-7

Olson, R. J., Chisholm, S. W., Zettler, E. R., & Armbrust, E. V. (1988, March). Analysis of *Synechococcus* pigment types in the sea using single and dual beam flow cytometry. *Deep Sea Research Part A. Oceanographic Research Papers, 35*(3), 425–440. https://doi.org/10.1016/0198-0149(88)90019-2

Paerl, H. W., & Huisman, J. (2009, February 5). Climate change: a catalyst for global expansion of harmful cyanobacterial blooms. *Environmental Microbiology Reports, 1*(1), 27-37. https://doi.org/10.1111/j.1758-2229.2008.00004.x

Palenik, B. (2001). Chromatic Adaptation in MarineSynechococcus Strains. *Applied and Environmental Microbiology*. https://doi.org/10.1128/AEM.67.2.991-994.2001

Partensky, F., Hess, W. R., & Vaulot, D. (1999a, March). Prochlorococcus, a marine photosynthetic prokaryote of global significance. *Microbiology and molecular biology reviews: MMBR*, *63*(1), 106–127. https://doi.org/10.1128/MMBR.63.1.106-127.1999

Partensky, F., Blanchot, J., & Vaulot, D. (1999b, July). Differential distribution and ecology of Prochlorococcus and Synechococcus in ocean waters: a review. *Bull Oceanography Monaco, 19*, 457–76.

Pick, F. R. (1991, November). The abundance and composition of freshwater picocyanobacteria in relation to light penetration. *Limnology and Oceanography, 36*(7), 1457-1462. https://doi.org/10.4319/lo.1991.36.7.1457

R Core Team. (2021). R: A language and environment for statistical computing. *R Foundation for Statistical Computing,* Vienna, Austria. https://www.R-project.org/

Ribalet, F., Berthiaume, C., Hynes, A., Swalwell, J., Carlson, M., Clayton, S., Hennon, G., Poirier, C., Shimabukuro, E., White, A., & Armbrust, E. V. (2019). SeaFlow data v1, high-resolution abundance, size and biomass of small phytoplankton in the North Pacific. *Scientific Data*, *6*(1), 277. https://doi.org/10.1038/s41597-019-0292-2

Robertson, B. R., Tezuka, N., & Watanabe M. M. (2001, May). Phylogenetic analyses of Synechococcus strains (cyanobacteria) using sequences of 16S rDNA and part of the phycocyanin operon reveal multiple evolutionary lines and reflect phycobilin content. *International Journal of Systematic and Evolutionary Microbiology, 51*(Pt 3), 861–871. https://doi.org/10.1099/00207713-51-3-861

Rose, J. M., & Caron, D. A. (2007). Does low temperature constrain the growth rates of heterotrophic protists? Evidence and implications for algal blooms in cold waters. *Limnology and Oceanography*, *52*(2), 886-895.

Sánchez-Baracaldo, P., Hayes, P. K., & Blank, C. E. (2005, December 19). Morphological and habitat evolution in the cyanobacteria using a compartmentalization approach. *Geobiology, 3*(3), 145 – 165. https://doi.org/10.1111/j.1472-4669.2005.00050.x

Sánchez-Baracaldo, P., Handley, B. A., & Hayes, P. K. (2008). Picocyanobacterial community structure of freshwater lakes and the Baltic Sea revealed by phylogenetic analyses and clade-specific quantitative PCR. *Microbiology*, *154*(11), 3347–3357. https://doi.org/10.1099/mic.0.2008/019836-0

Sanders, R. W., Berninger, U. G., Lim, E., L., Kemp, P. F., & Caron, D. A. (2000, January 31). Heterotrophic and mixotrophic nanoplankton predation on picoplankton in the Sargasso Sea and Georges Bank. *Marine Ecology Progress Series, 192*, 103-118. http://dx.doi.org/10.3354/meps192103

Scanlan, D. J., & West, N. J. (2002, April). Molecular ecology of the marine cyanobacterial genera *Prochlorococcus* and *Synechococcus*. *FEMS Microbiology Ecology, 40*(1), 1-12. https://doi.org/10.1111/j.1574-6941.2002.tb00930.x

Scanlan, D. J. (2012). Marine Picocyanobacteria. In: Whitton, B. A., & Potts, M. (eds) The ecology of cyanobacteria II. Dordrecht, The Netherlands: *Springer, 2nd,* 503–533. https://doi.org/10.1007/978-94-007-3855-3

Six, C., Thomas, J.-C., Thion, L., Lemoine, Y., Zal, F., & Partensky, F. (2005). Two Novel Phycoerythrin-Associated Linker Proteins in the Marine Cyanobacterium Synechococcus sp. Strain WH8102. *Journal of Bacteriology*, *187*(5), 1685. https://doi.org/10.1128/JB.187.5.1685-1694.2005

Six, C., Thomas, J., Garczarek, L., Ostrowski, M., Dufresne, A., Blot, N., Scanlan, D. J., & Partensky, F. (2007, December 5). Diversity and evolution of phycobilisomes in marine *Synechococcus spp.*: a comparative genomics study. *Genome Biology, 8,* article no. R259–R259. https://doi.org/10.1186/gb-2007-8-12-r259

Sswat, M., Stiasny, M. H., Taucher, J., Algueró-Muñiz, M., Bach, L. T., Jutfelt, F., Riebesell, U., & Clemmesen, C. (2018). Food web changes under ocean acidification promote herring larvae survival. *Nature Ecology & Evolution*, *2*(5), Article 5. https://doi.org/10.1038/s41559-018-0514-6

Stockner, J. G., & Antia, N. J. (1986, December). Algal Picoplankton from Marine and Freshwater Ecosystems: A Multidisciplinary Perspective. *Canadian Journal of Fisheries and Aquatic Sciences, 43,* 2472-2503. https://doi.org/10.1139/f86-307

Stockner, J.G. (1988, July). Phototrophic picoplankton: An overview from marine and freshwater ecosystems. *Limnology and Oceanography, 33*(4, part 2), 765–775. https://doi.org/10.4319/lo.1988.33.4part2.0765

Stockner, J., Callieri, C., & Cronberg, G. (2000). Picoplankton and Other Non-Bloom-Forming Cyanobacteria in Lakes. In: Whitton, B. A., & Potts, M. (eds) The ecology of cyanobacteria. The Netherlands*: Springer, 7,* 195–231. https://doi.org/10.1007/0-306-46855-7_7

Stomp, M., Huisman, J., de Jongh, F., Veraart, A.J., Gerla, D., Rijkeboer, M., Ibelings, B. W., Wollenzien, U. I. A., & Stal, L. J. (2004, October 10). Adaptive divergence in pigment composition promotes phytoplankton biodiversity. *Nature, 432*, 104–107. https://doi.org/10.1038/nature03044

Stomp, M., Huisman, J., Vörös, L., Pick, F. R., Laamanen, M., Haverkamp, T., & Stal, L. J. (2007). Colourful coexistence of red and green picocyanobacteria in lakes and seas. *Ecology Letters*, *10*(4), 290–298. https://doi.org/10.1111/j.1461-0248.2007.01026.x

Sullivan, B. E. (1997). Annual Cycles of Organic Matter and Phytoplankton Attributes in the Columbia and Willamette Rivers, with Reference to the Columbia River Estuary. *MSc thesis submitted to Oregon State University.*

Sullivan, B. E., Prahl, F. G., Small, L. F., & Covert, P. A. (2001). Seasonality of phytoplankton production in the Columbia River: A natural or anthropogenic pattern? *Geochimica et Cosmochimica Acta*, *65*(7), 1125–1139. https://doi.org/10.1016/S0016-7037(00)00565-2

Sun, J., Lin, J., Zhang, X., Xiao, Z., Lin, B., & Xu, H. (2021, February 22). Dam-influenced seasonally varying water temperature in the Three Gorges Reservoir. *River Research and Applications, 37*(4), 579-590. https://doi.org/10.1002/rra.3780

Swanson, H. A., & Baldwin, H. L. (1965). A Primer on Water Quality*. U.S. Geological Survey.* https://pubs.usgs.gov/fs/fs-027-01/pdf/FS-027-01.pdf

Thompson, A. W., & Engh, G. van den. (2016). A multi-laser flow cytometry method to measure single cell and population-level relative fluorescence action spectra for the targeted study and isolation of phytoplankton in complex assemblages. *Limnology and Oceanography: Methods*, *14*(1), 39–49. https://doi.org/10.1002/lom3.10068

Urbach, E., Scanlan, D. J., Distel, D. L., Waterbury, J. B., & Chisholm, S. W. (1998, February). Rapid diversification of marine picophytoplankton with dissimilar light-harvesting structure inferred from sequences of Prochlorococcus and Synechococcus (Cyanobacteria). *Journal of Molecular Evolution, 46*(2), 188-201. https://doi.org/10.1007/pl00006294

U.S. Geological Survey (USGS). (1990, May). Water Fact Sheet: Largest Rivers in the United States. *U.S. Department of the Interior*. https://pubs.usgs.gov/of/1987/ofr87-242/pdf/ofr87242.pdf

Vörös, L., Callieri, C., Katalin, V., & Bertoni, R. (1998, May). Freshwater picocyanobacteria along a trophic gradient and light quality range. *Hydrobiologia, 369*, 117-125. https://doi.org/10.1023/A:1017026700003

Ward, B. A., Dutkiewicz, S., Jahn, O., & Follows, M. J. (2012). A size structured food-web model for the global ocean. *Limnology and Oceanography, 57*, 1877–1891. https://doi.org/10.4319/lo.2012.57.6.1877

Wawrik, B., & Paul, J. H. (2004, April). Phytoplankton Community Structure and Productivity Along the Axis of the Mississippi River Plume in Oligotrophic Gulf of Mexico Waters. *Aquatic Microbial Ecology, 35*(2), 185–196. http://dx.doi.org/10.3354/Ame035185

Wickham, H. (2016). ggplot2: Elegant Graphics for Data Analysis. *Springer*, Verlag, New York. https://ggplot2.tidyverse.org

Williams, R. J. P. (1997). The natural selection of the chemical elements. *Cellular and Molecular Life Sciences CMLS*, *53*, 816-829.

Winder, M. (2009). Photosynthetic picoplankton dynamics in Lake Tahoe: Temporal and spatial niche partitioning among prokaryotic and eukaryotic cells. *Journal of Plankton Research*, *31*(11), 1307–1320. https://doi.org/10.1093/plankt/fbp074

Wood, A. M., Horan, P. K., Muirhead, K., Phinney, D. A., Yentsch, C. M., & Waterbury, J. B. (1985, November). Discrimination between types of pigments in marine Synechococcus spp. by scanning spectroscopy, epifluorescence microscopy and flow cytometry. *Limnology and Oceanography, 30*(6), 1303-1315. https://doi.org/10.4319/lo.1985.30.6.1303

Worden, A. Z., Nolan, J. K., & Palenik, B. (2004, January 31). Assessing the dynamics and ecology of marine picophytoplankton: The importance of the eukaryotic component. *Limnology and Oceanography, 49*(1), 168-179. https://doi.org/10.4319/lo.2004.49.1.0168

Zwirglmaier, K., Jardillier, L., Ostrowski, M., Mazard, S., Garczarek, L., Vaulot, D., Not, F., Massana, R., Ulloa, O., & Scanlan, D. (2008, January 10). Global phylogeography of marine Synechococcus and Prochlorococcus reveals a distinct partitioning of lineages among oceanic biomes. *Environmental Microbiology, 10*(1), 147-161. https://doi.org/10.1111/j.1462-2920.2007.01440.x

Appendix A. Raw master data spreadsheet

Name: 2023_11_27_MasterData

File Type: Microsoft Excel Comma Separated Values File

Size: 12 KB

Required Application Software: Microsoft Excel

Description:

The raw “Master Data” file for this project contains the following sample information in order by column. A) The sample ID with letters ‘C’ and ‘W’ indicating Columbia and Willamette samples, respectively. B) The corresponding sample location. C) The sample date. D) The sample time, rounded to the nearest 15-minute increment. E) The average daily temperature reading (°C) retrieved from USGS. F) The turbidity readings (FNU) at that exact date and time, retrieved from USGS. G) The average daily discharge readings (cfs) retrieved from USGS. H) The nitrate readings (mg per L of nitrogen) at that exact date and time, retrieved from USGS (only available for the Willamette River). I) The date samples were flow cytometrically analyzed. J) The type of internal polystyrene microsphere (bead) standard based on diameter size (µm) and fluorescence (UR = Ultra Rainbow, YG = Yellow Green). K) The calculated flow rates (mL per s) correspond to each sample analysis date. L) The time each sample was ran (seconds). M) The sample volume (mL) calculated from the flow rate and run time of samples. N-X) The raw event count for the ungated sample, chlorophyll-containing cells gate including the beads, the chlorophyll-containing cells negatively gating the beads, the beads gate, and CP4, C1, CP1, CP3, CP2, C2, and P1 gates. Y-AH) The respective concentrations (cells per mL) of columns N-X calculated by dividing by the sample volume.

Appendix B. Chlorophyll-positive gates

Name: 2023_10_17_CHLgateBatch

File Type: Adobe Acrobat Document

Size: 1,195 KB

Required Application Software: Adobe Acrobat

Description:

This file demonstrates the gating scheme used for grouping chlorophyll-containing (chlorophyll positive) events. Each density dot plot represents a different sample taken from either the Columbia or Willamette River, annotated along the bottom of each plot by the raw file name. Raw file names consist of the analyzed date followed by the sample ID, for example the first plot is sample ID W004 analyzed on December 20, 2022. The colored dots represent individual particles that range from dark blue to red, representing a low and high frequency of events, respectively. Events are plotted based on their relative chlorophyll fluorescence and forward light scatter detection, both excited by the 488 nm laser, to distinguish cells of the appropriate size range that contain chlorophyll.

Appendix C. Chlorophyll fluorescence needles

Name: 2023_12_03_CHLcolorcodedBatch

File Type: TIFF File

Size: 1,439 KB

Required Application Software: Windows Photo Viewer

Description:

This file illustrates the seven populations identified plotted on bivariate relative chlorophyll fluorescence plots. Each color-coded dot plot represents a different sample taken from either the Columbia or Willamette River, annotated along the bottom of each plot by the raw file name. Raw file names consist of the analyzed date followed by the sample ID, for example the first plot is sample ID W004 analyzed on December 20, 2022. The colored dots represent the cells that make up the seven different populations outlined in Figure 4, with the grey events representing a combination of beads and background noise. Events are plotted based on their relative chlorophyll fluorescence excited by the 488 and 561 nm lasers to assess characteristic chlorophyll fluorescence ratios of picophytoplankton populations.

Appendix D. Phycoerythrin fluorescence needles

Name: 2023_12_03_PEcolorcodedBatch

File Type: TIFF File

Size: 1,484 KB

Required Application Software: Windows Photo Viewer

Description:

This file illustrates the seven populations identified plotted on bivariate relative phycoerythrin fluorescence plots. Each color-coded dot plot represents a different sample taken from either the Columbia or Willamette River, annotated along the bottom of each plot by the raw file name. Raw file names consist of the analyzed date followed by the sample ID, for example the first plot is sample ID W004 analyzed on December 20, 2022. The colored dots represent the cells that make up the seven different populations outlined in Figure 4, with the grey events representing a combination of beads and background noise. Events are plotted based on their relative phycoerythrin fluorescence excited by the 488 and 561 nm lasers to assess characteristic phycoerythrin fluorescence ratios of picophytoplankton populations.

Appendix E. Trophic interactions co-authorship

Name: Ubiquitous filter feeders shape open ocean microbial community structure and function

File Type: PDF Document

Size: 1,621 KB

Required Application Software: Adobe Acrobat

Description:

This paper has been published in PNAS Nexus. My contributions as a co-author include performing and writing about the flow cytometric analysis. Specifically, I processed around 30 raw seawater samples to produce cell count data. The data I produced was used to calculate clearance rates of filter-feeding, gelatinous grazers on different picophytoplankton prey. These clearance rates were an integral part of the research, informing modeling and qPCR approaches. From there, I drafted the flow cytometric methodology section and provided suggestions and feedback throughout the writing process. Findings from this paper illuminate the relationships between microbial prey and gelatinous grazers in marine ecosystems. We showed that selective feeding was performed by one type of gelatinous grazer called salps. The salps studied rejected *Prochlorococcus* (the most abundant picocyanobacterium) and SAR11 during feeding while consuming other primary producers like *Synechococcus* and diatoms. This escape from predation by *Prochlorococcus* and SAR11 could not be explained by size alone, thus highlighting that novel microbial mechanisms for evading predation are likely at play.

Thompson, A. W., Nyerges, G., Brevick, K., & Sutherland, K. R. (2023). Ubiquitous filter feeders shape open ocean microbial community structure and function. *PNAS*. [Manuscript submitted for publication]